Archives of Civil and Mechanical Engineering (2023) 23:178
https://doi.org/10.1007/s43452-023-00720-9

ORIGINAL ARTICLE

Statistical model analysis of typical bridges considering the actual seismic damage observation database

Si-Qi Li[1,2,3] · Antonio Formisano[4]

Received: 16 March 2023 / Revised: 9 June 2023 / Accepted: 11 June 2023 / Published online: 24 June 2023

Abstract
To study the seismic vulnerabilities and performances of typical bridges, data from a field investigation of 2134 bridges on 22 highway sections hit by the Wenchuan earthquake that occurred in China on May 12, 2008, were collected and processed. From the sample data of the empirical seismic-damage observations, 1409 simply supported girder bridges, 107 continuous girder bridges, and 612 arch bridges were selected. The latest version of the Chinese seismic intensity standard was utilized to evaluate the fragility of bridge samples in different macroseismic intensity zones, and the empirical vulnerability matrix and multidimensional regression comparison model of typical bridge clusters were developed. Taking the bridge length, the coordinate azimuth of the bridge location, the number of spans, the geometric form of the pier columns, and the type of bearings and foundations as the single factors influencing vulnerability and assuming (i) the line type and bridge length, (ii) the types of pier column and foundation, and (iii) the number of spans, the type of bearings, foundations, and linearity as the coupled factors influencing vulnerability, the aforementioned typical bridges were subjected to comparative vulnerability analysis. Innovative fragility regression and probability comparison models of typical bridges were developed considering the influence of multiple factor coupling. A novel vulnerability evaluation model was proposed based on the characteristic parameters and damage grade of bridge clusters in the umbrella earthquake area, and the model was optimized and verified by using the typical bridge database of the Wenchuan earthquake.

Keywords Typical bridge · Empirical seismic vulnerability · Comparative analysis · Single and coupling factors · Innovative failure probability model

Abbreviations

PGA	Peak ground acceleration
PGV	Peak ground velocity
SSG	Simply supported girder bridge
CG	Continuous girder bridge
AB	Arch bridge
OAB	Ordinary
DAB	Double curvature
DTRA	Deck-type ribbed
MPAB	Masonry plate
RCBA	RC box

✉ Si-Qi Li
lisiqi@hlju.edu.cn

Antonio Formisano
antoform@unina.it
https://scholar.google.com/citations?user=clr8ggIAAAAJ&hl=it

1 School of Civil Engineering, Heilongjiang University, No. 74, Xuefu Road, Harbin City, China

2 Longjian Road and Bridge Co., Ltd, No. 109, Songshan Road, Harbin City, China

3 School of Transportation Science and Engineering, Harbin Institute of Technology, Harbin City, China

4 Department of Structures for Engineering and Architecture, School of Polytechnic and Basic Sciences, University of Naples "Federico II", Naples, Italy

SSAB	Semisupported
RCPA	RC plate
RCRA	RC rib
SC	Simply supported and continuous girder
SB	Suspension
CSB	Cable-stayed bridge
DS	Damage state
DS1	Intact
DS2	Mildly damaged
DS3	Moderately damaged
DS4	Heavily damaged
DS5	Destruction
FI	Failure index
VG	Vulnerability grade
VCFM	Vulnerability curve fit model
ACFP	Actual cumulative failure-exceeding probability
GRM	Gaussian regression model
ULDM	Updated lognormal distribution model
CSIS	Chinese seismic intensity standard
IM	Intensity measure
BL	Bridge length
VSS	Vulnerability survey sample
GQFM	Gauss quadratic fitting model
CA	Coordinate azimuth
S	Span
PT	Pier type
OT	Other bridge
P1	Bent piers
P2	Single-column piers
P3	Rectangular thin-walled piers
P4	Masonry entity piers
P5	Composite piers
P6	Other piers
N/A	Single span without piers
FT	Foundation type
F1	Expansion foundation
F2	Pile foundation
F1 + F2	Mixed foundation
BT	Bearing type
B1	Laminated rubber bearings
B2	Basin rubber bearings
B3	Other bearings
B4	No bearings
L	Linear type
SL	Straight-line
CL	Curved-line
GFFM	Gaussian first-fit model

1 Introduction

Over the years, earthquakes worldwide have had far-reaching impacts on people; in particular, house collapses and damage to infrastructure and the ground have affected people's production and lives either directly or indirectly and have caused many casualties and much loss of property. Bridge structures are not only essential lifeline projects but also infrastructure that supports the transportation network for emergency rescue and disaster relief after an earthquake. Earthquakes of differing intensities will damage different types of bridges to varying degrees, and the degree of damage is related directly to the bridge's use function. Therefore, the study of bridge seismic vulnerability has practical application significance. According to (i) many global reports on historical earthquake disasters involving moderate and strong earthquakes and (ii) field-observation data on seismic damage, the damage to various bridges in multiple-intensity regions is relatively significant, and some bridges even partially or completely collapse in higher-intensity regions. To further study the earthquake performance of typical bridges and analyze their fragility under different seismic loads, experts in seismic engineering around the world have researched the vulnerability of bridge structures.

Part of that research has involved combining seismic demand models [1] with related theories to analyze the vulnerability of bridges. Shekhar and Ghosh [2] proposed a multidimensional model based on life-cycle cost assessment for the fragility of highway bridges and used it to assess the vulnerability (earthquake damage probability) of typical highway concrete simply supported girder bridges in the central and southeastern United States. Considering asynchronous dynamic response and soil–structure interaction, Ramadan et al. [3] selected a nine-span continuous box-girder bridge subjected to incremental dynamic analysis to obtain its vulnerability curve based on the probability of exceedance. Li et al. [4] studied the interface friction and damage internal friction in the bridge structure system so that the research results were applied for the seismic design of bridge bearings. Perdomo et al. [5] used the capacity spectrum and pushover analysis to analyze the vulnerability of a typical Italian reinforced concrete (RC) bridge; combined with a probabilistic earthquake demand model, they established the model-exceeding probability and vulnerability curve of earthquake measures under different fragility grades. Cademartori et al. [6] analyzed the vulnerability of typical RC bridges in Italy with the input parameters of displacement capacity as a vector, and they classified the vulnerability curves of bridges more accurately. Using survey samples of traffic bridges in the central and southeastern United States, Padgett and Desroches [7] performed a vulnerability analysis of local bridge components using probabilistic demand-model theory; they provided vulnerability-curve models, proposed a vulnerability assessment model based on various reinforcement measures, drew vulnerability curves, and showed that the piers, abutments, and bearings of bridges are damaged relatively prominently under earthquakes. Considering the seismic intensity measure (peak ground acceleration (PGA)), ground motion duration, structural geometric properties, sensitivity parameter, soil conditions, and site characteristics as the research objects and combining them with a vulnerability probability model, Li and Liu [8] developed models of vulnerability probability curves, fragility lines, and functions. Through the impact on typical sources of uncertainty, Soleimani [9] analyzed the seismic vulnerability of rare and common box girders based on different ground motion parameters (PGA and peak ground velocity), materials, and geometric forms, developed a probabilistic seismic demand model, and generated vulnerability curves. However, field seismic damage investigations have shown that the length, coordinate azimuth of bridge location, span number, bearing, foundation, and linear structure have a significant impact on the fragility of various bridges, and there is relatively little research on these vulnerability impact factors.

With computer numerical simulation and experimental technology development, bridge research involving finite-element seismic simulations and shaking-table tests progressed considerably. Bhuiyan and Alam [10] selected a three-span continuous highway bridge for two-dimensional finite-element modelling, used incremental dynamic analysis to analyze the earthquake vulnerability of its piers and bearings, and gave the relationship between the bridge vulnerability curve and the peak ground acceleration (PGA). Kappos et al. [11] established a finite-element model for a four-span highway bridge with piers of unequal heights, analyzed the dynamic time histories of its slab, pier, and carriageway foundation, and evaluated the seismic capacity of each component. Taking a typical continuous flyover as their example, Agalianos et al. [12] established a three-dimensional finite-element model, analyzed the geometric nonlinear relationship among the bridge, foundation, and soil system, and obtained the damage characteristics of the bridge affected by a fault. Tong et al. [13] conducted shaking-table tests on rectangular concrete piers strengthened with high-performance materials and obtained the vulnerability of the piers under different ground motions (earthquake moment magnitude (Mw), PGA, seismic record station, and PGV). Regarding a real bridge, Attary et al. [14] made a reduced-scale model with four damping devices, conducted shaking-table tests, and analyzed the seismic vulnerability of bridges with different damping devices. However, it is relatively rare to evaluate the seismic vulnerability of a regional group of typical bridges using the macroseismic intensity.

Studying bridge vulnerability judgmental or expert-based, empirical, and numerical methods [15] can effectively and directly evaluate the seismic loss of actual bridges. Lew et al. [16] collected data on bridges damaged in typical earthquakes in New Zealand between 1968 and 2016; they analyzed the vulnerability of bridges with PGA as the seismic measure parameter, and they obtained the vulnerability characteristics of bridges under different PGA actions. Li et al. [17] statistically analyzed the data of typical highway bridges in eastern China, developed the vulnerability curves of bridges in local areas, and provided vulnerability models for different types of bridges. Padgett et al. [18] collected data on 375 bridges in the Charleston area of the United States, used a model that combined seismic risk and the vulnerability curve to analyze the vulnerability in empirical data [19], and predicted and assessed the potential vulnerability and economic loss of each bridge. However, although subjecting vulnerability to theoretical and finite-element analyses and vibration tests can calculate the dynamic response of a bridge structure accurately and evaluate its seismic damage vulnerability, it is difficult to evaluate the vulnerability of all types of bridge structures in a specific or overall seismic region. Empirical fragility analysis is based on the actual situation of bridge earthquake loss, which can solve this problem, but because of the huge workload and cost of sample research, there has been relatively little research in this area.

Additionally, the author's early work [20] combined multidimensional analysis of actual seismic damage data of building [21] and bridge structures [22] and developed a calculation method to evaluate the vulnerability of typical buildings and bridges using traditional nonlinear fitting models [23]. However, these works overlook the damage modes and vulnerability characteristics of regional bridges affected by various factors. Therefore, the quantification accuracy of the probability model established to evaluate the vulnerability of typical bridge clusters is relatively low. This study focuses on the shortcomings of the established model and considers the impact of various influencing factors on the seismic vulnerability of bridges. It innovatively proposes an empirical vulnerability probability model that considers the influence of multiple individual and coupling factors and optimizes and verifies the model using actual seismic damage bridge data from three provinces in China.

To relatively precisely assess the fragility of all types of typical bridges in a typical earthquake, the present study involved collecting and collating seismic-damage survey data on 2134 bridges damaged in the Wenchuan earthquake in China. A fragility analysis was performed based on the empirical seismic-damage survey data samples. The Chinese seismic intensity standard [24] was used to assess the vulnerability level of bridge samples in different macrointensity regions, and the empirical vulnerability matrix and multidimensional regression comparison model of typical bridges were established. A novel vulnerability evaluation model was proposed based on the characteristic parameters and damage grade of bridge clusters in the overall earthquake zone, and the model was optimized and verified by using the typical bridge database of the Wenchuan earthquake. It was found that in the whole area affected by the Wenchuan earthquake, the vulnerability of bridges of different lengths, coordinate azimuth of bridge location, span number, bearing, foundation, and linear structure differed significantly. Therefore, the aforementioned vulnerability factors were subjected to single and coupled response analyses based on the actual seismic-damage survey data. The fragility curve models of simply supported girder bridges (SSGs), continuous girder bridges (CGs), and arch bridges (ABs) based on quantity and failure probability were established under different influencing factors, and a comparative analysis was conducted. The research results obtained could provide a reasonable reference for reviewing intensity zoning and verifying macroseismic intensity levels in bridge failure assessment.

2 Survey of highway bridges hit by the Wenchuan earthquake

To study the seismic fragility of various engineering structures, from May to October 2008, after the Wenchuan earthquake, the China Earthquake Administration, the Ministry of Communications, scientific research institutes, universities, and earthquake engineering and anti-seismic experts and scholars from around the world formed relevant field investigation groups that went successively to relevant seismic regions according to the distribution of Wenchuan seismic

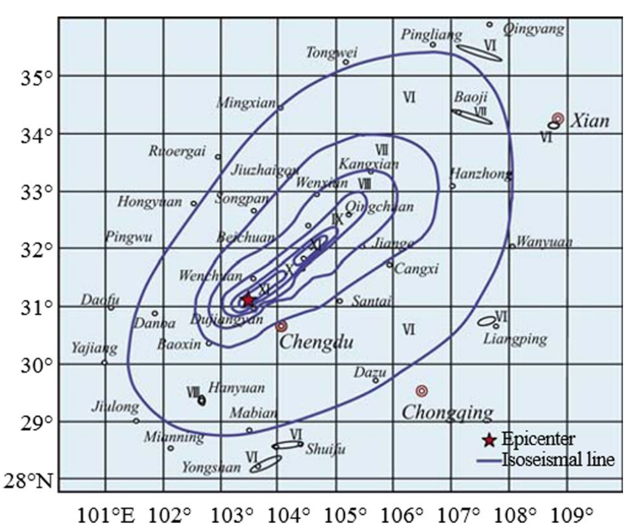

Fig. 1 Macrointensity map of Wenchuan earthquake in China. [27]

intensity issued by the China Earthquake Administration, as shown in Fig. 1 [25], and seismic-damage field observations of engineering structures were made in different regions. According to the investigation data of each engineering-structure reconnaissance group, bridge structures were damaged to different degrees during the earthquake, which greatly hindered the rescue work in the earthquake area. To understand the overall damage situation of typical bridges in the seismic region and analyze the seismic performance of various typical bridges, in this study, based on the empirical seismic-damage investigation data of the first author's investigation team and other teams, seismic-damage observation data on 2134 bridges on 22 highways (JKGS, HRGS, XRGS, CYGS, CDGS, DJYGS, S105, S106, G108, S205, S209, S210, S211, G212, G213, S301, S302, S303, S306, S309, G317, and G318) Sects. (47 subsections) in the provinces of Sichuan, Gansu, and Shaanxi (provinces with heavy bridge damage caused by the Wenchuan earthquake) were collected and processed for comparative analysis of the vulnerability of typical bridges. The core purpose of this study was to evaluate the vulnerability characteristics of typical groups of bridges in a monolithic seismic area. New fragility analysis was performed with the macroseismic scale as an intensity measure, and the failure features, specific local site conditions, seismic design requirements, and input motions (PGAs) of bridges in each intensity zone were not considered. Figure 2 depicts the distribution of highway and bridge samples and the statistics of bridge samples in each section of these sample reconnaissance areas. The types of bridges in the earthquake area varied, comprising mainly SSG, CG, AB ((ordinary (OAB), double curvature (DAB), deck-type ribbed (DTRA), masonry plate (MPAB)), RC box (RCBA), semisupported (SSAB), RC plate (RCPA), and RC rib (RCRA)), simply supported and continuous girder (SC), suspension (SB), and cable-stayed bridges (CSB). The bridge's seismic damage observation region and vulnerability grade were defined according to GB/T 17742-2020 and GB/T 24336-2009 (China) standards [26], and the macrointensity level was IV or above (PGA $\geq$ 0.22 g). The numbers of bridges investigated in the seismic regions are depicted in Fig. 3a. Because of the diversity of AB structure types in the investigation area, statistics were prepared on the various AB types, as reported in Fig. 3b.

According to the survey data, 2128 SSG, CG, and AB bridges accounted for 99.7% of the total sample. To a certain extent, these three types of bridges have a huge stock and a wide range of applications. Therefore, subjecting these three types of bridges to comparative vulnerability analysis has practical significance.

According to the seismic damage classification of lifeline engineering (GB/T 24336-2009, China) [26], the bridge seismic code (JTG/T B02-01-2008 [28], JTG/T 2231-01-2020 [29], China) and the Chinese seismic intensity standard

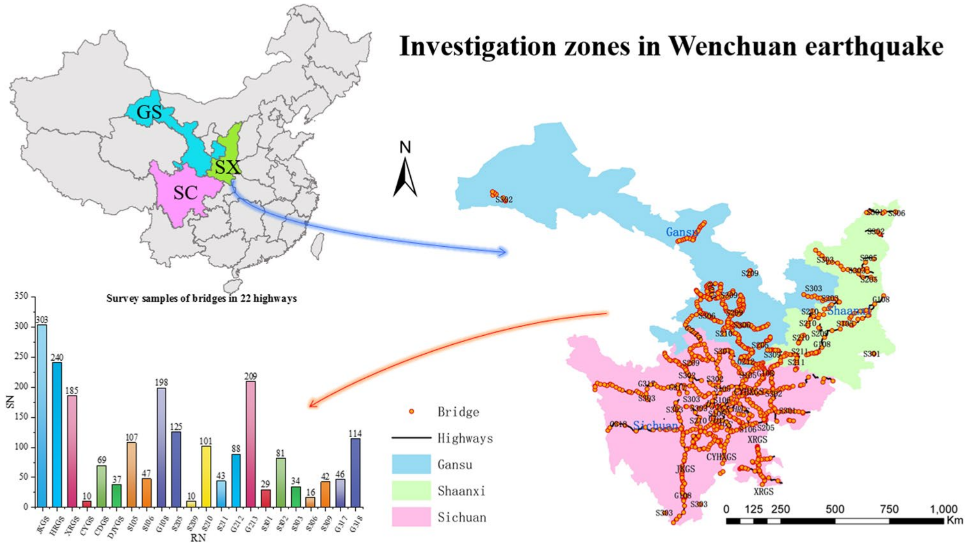

Fig. 2 Sample distribution of reconnaissance regions for roads and bridges [32]

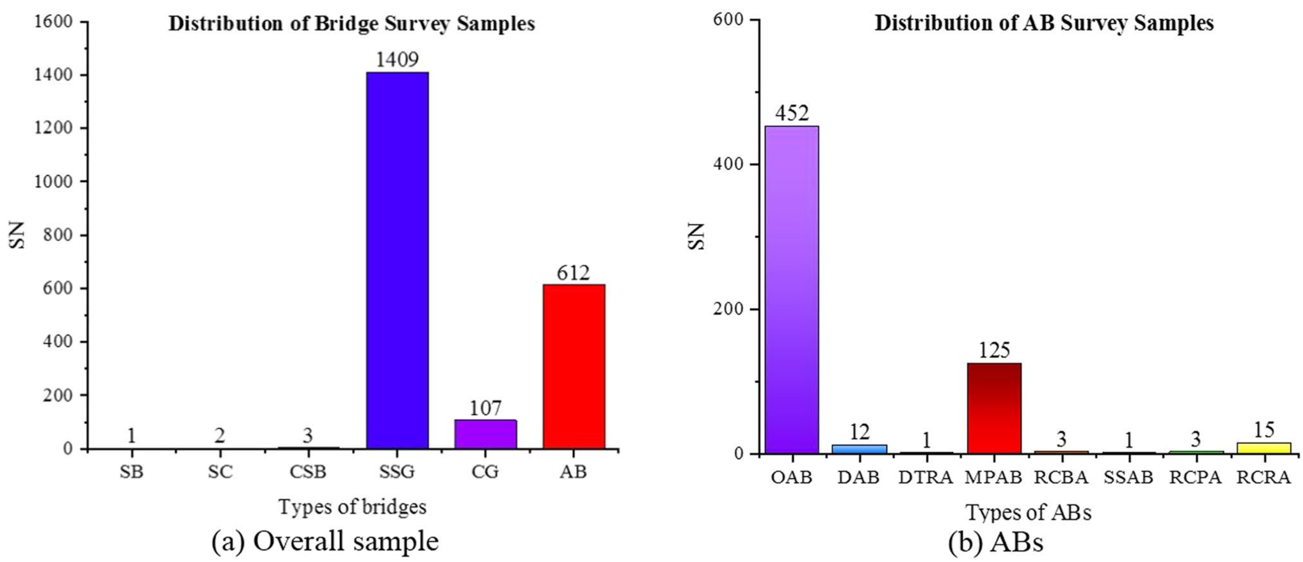

Fig. 3 Distribution of samples of various bridges in the survey area (SN = sample number)

[30], the bridge seismic-damage investigation team assessed the vulnerability of SSG, CG, and AB samples in the Wenchuan earthquake field observation zone. Table 1 lists the detailed standards for assessing the vulnerability levels of the three types of bridges, and it classifies the vulnerability levels (damage state (DS)) of the various types of bridges into five levels (intact (DS1), mildly damaged (DS2), moderately damaged (DS3), heavily damaged (DS4), and destruction (DS5)) [31]. The relationship between the damage and vulnerability level of the bearing and nonbearing components of a bridge was established as a guiding principle for the bridge investigation group to carry out the reconnaissance work of various types of bridge earthquake damage.

Among the many research results of vulnerability that have been obtained, the PGA was commonly used as a ground motion parameter to establish the relationship model of the bridge damage ratio or exceedance probability. To accurately obtain the seismic damage characteristics of typical bridge vulnerability under multiple vulnerability levels, this study takes the vulnerability level (DS1–DS5) as the quantitative evaluation parameter, and vulnerability correlation models between this parameter and the failure index and actual cumulative failure-exceedance probability are established from another dimension.

According to the vulnerability assessment criteria for bridges, the vulnerability grades of SSG, CG, and AB were assessed, and the sample statistics were gathered. The

Table 1 Standards for assessing the seismic damage of bridges with different vulnerability grades (GB/T 24336-2009, Classification of earthquake failure to lifeline engineering, China)

Vulnerability level	Details of seismic failure assessment
Intact (DS1)	No damage to structural members of the bridge; inconspicuous deformation of bridge deck; individual nonstructural members may be damaged. Continue to use without repair
Mildly damaged (DS2)	There is no seismic damage to load-bearing components such as bridge deck, abutments, piers, arches, towers, and main beams; local surface concrete peeling, guardrails, expansion joints, abutment cone slopes, and other non-bearing components are damaged, and the support connection parts are slightly deformed. A bridge can pass with either no or slight repair
Moderately damaged (DS3)	Remarkable cracks in pier concrete, but no apparent inclination; the protective layer has peeled off, but the concrete in the core area is not damaged, and the bearing capacity of the piers has decreased significantly; cracks in the concrete at the bridge ends; displacement of main girders, but there is still reliable support and no risk of falling beams. Abutments are slightly damaged, and their back and wing walls are cracked. The transverse connection of the arch bridge is cracked, and the column on the arch is slightly cracked
Heavily damaged (DS4)	Serious displacement of main girders, but they can still be supported reliably without falling-beam risk; there are obvious through cracks or multiple shear joints in the pier concrete, which extend to the core area, peel off, and seriously crack and incline; abutments are damaged, back and wing walls are seriously cracked or collapsed, and abutment caps (cap beam) are cut. The main arch ring of the arch bridge is transversely penetrated and cracked, and the column on the arch is broken, as is the transverse connection
Destruction (DS5)	Either the whole bridge or part of its span units has collapsed as a whole, the fallen beams, piers, and abutments are broken or may collapse at any time, and the piers are crushed or sheared

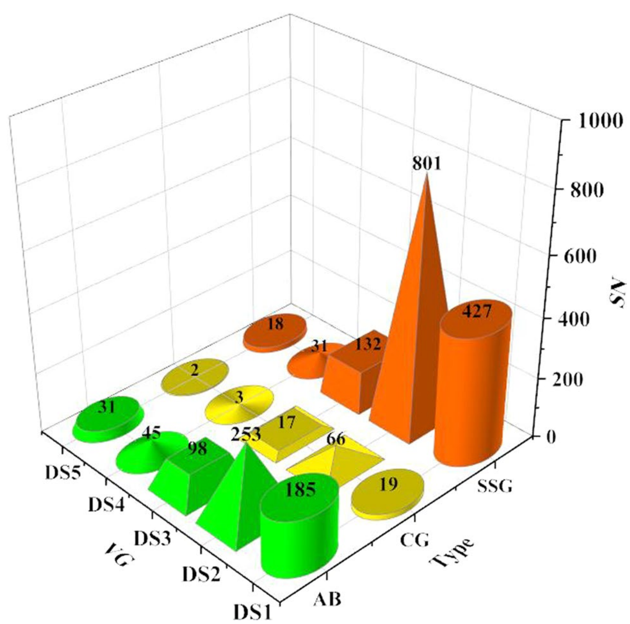

Fig. 4 Field observation samples of typical bridges under multiple vulnerability grades (VGs)

Table 2 Fragility matrix model of seismic damage considering the failure index (FI, number of bridge samples with different vulnerability levels divided by the total number) [%]

Type	Vulnerability level				
	DS1	DS2	DS3	DS4	DS5
SSG	30.3	56.8	9.4	2.2	1.3
CG	17.8	61.7	15.9	2.8	1.8
AB	30.2	41.3	16	7.4	5.1

statistical distribution of the vulnerability quantities of the three typical bridge types and the fragility matrix model based on the failure index (FI) were obtained, as depicted in Fig. 4 and Table 2.

To comprehensively compare the fragility of typical bridges in the holistic earthquake intensity region, the innovative vulnerability comparison plane and surface diagrams of three types of typical bridges are generated by using two-dimensional and three-dimensional numerical Mohr modal calculation methods, as presented in Fig. 5 a, b. A fragility trend model was obtained by applying numerical regression analysis and a probability model to the sample data. The sample points (SPs) were regressed by using an updated interpolant shape-preserving method (PCHIP, piecewise cubic Hermite interpolating polynomial) and empirical cumulative probability-exceeding model analysis, and the vulnerability curve fit model (VCFM) based on FI and the actual cumulative failure-exceeding probability (ACFP) was obtained, as presented in Fig. 5c, d. Notably, the goodness of fit of the PCHIP interpolation model is equal to 1. Compared with other interpolation models, the advantage of the PCHIP interpolation model is that it can more intuitively and vividly indicate the damage characteristics of different types of actual earthquake damage to bridge clusters. It is worth emphasizing that the ACFP corresponding to DS1 (Fig. 5d) is calculated by dividing the number of bridges at the DS1 level by the total number of bridges in the sample database.

According to the analysis of the empirical seismic-damage observation data of typical bridges, the sample number of SSG is significantly greater than that of CG and AB;

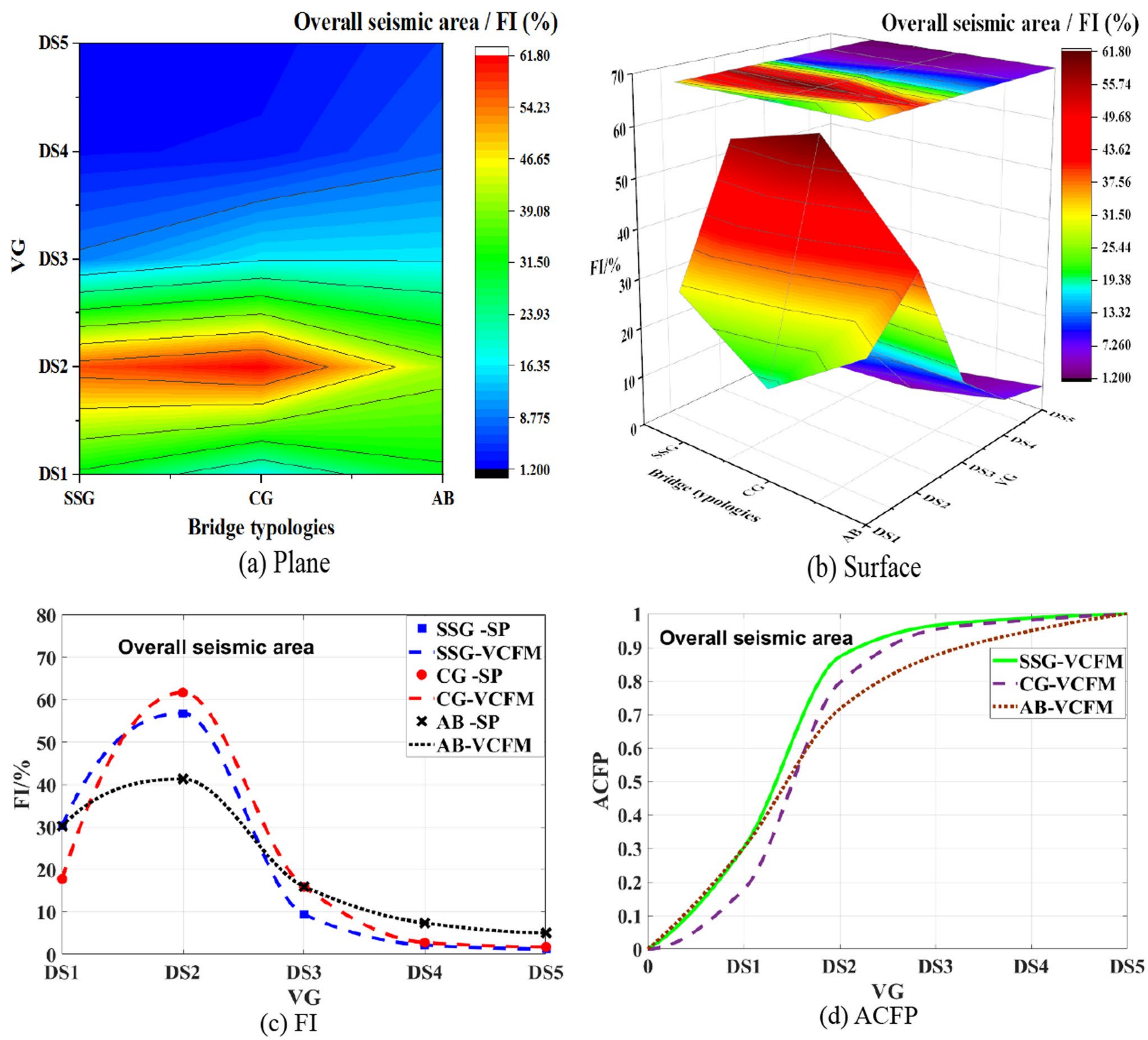

Fig. 5 Comparison of vulnerability models of simply supported girder bridges (SSG), continuous girder bridges (CG), and arch bridges (AB)

considering the vulnerability, this type of bridge is damaged significantly less than are the other two types. AB failure is more serious than that of SSG and CG, especially in DS4 and DS5. The damage of the SSG is slightly lighter than that of the CG, which is reflected mainly in the DS3 level. Note that the proportion of DS2 in each typical bridge is relatively large, which to a certain extent shows that the bridges basically achieved the seismic target of not collapsing in a large amount. However, we should focus on improving the integrity and ductility of all types of bridges, increasing the stiffness and strength of nonload-bearing components, and making the sample size of DS2 grade transfer to DS1 reasonably to achieve the goal of comprehensively improving the seismic capacity of bridges.

3 Vulnerability comparison model of typical bridge clusters in different seismic intensity zones

Empirical seismic vulnerability is an essential method to evaluate and predict the damage features of regional bridges under different intensity measures. Risk, reliability, and probability analysis methods are ubiquitously used to assess bridge seismic vulnerability. The transcendental probability theory and exponential model of structural damage were used by Formisano and Chieffo [33]. An exponential regression model (ERM) considering PGA and structural damage grade was established. An exponential regression curve was generated to predict the vulnerability of buildings, and the empirical vulnerability data of the L'Aquila earthquake in Italy were analyzed by nonlinear fitting. Chieffo et al. [34] used cumulative distribution function theory to propose a Gaussian regression model (GRM) to assess the vulnerability of regional buildings and verified the rationality by using the field survey data of typical earthquakes.

The above research and work have contributed significantly to the field of empirical vulnerability and promoted the development of this field. Based on the above methods, this study optimizes the traditional lognormal distribution function and develops an updated lognormal distribution model (ULDM) that can be used to suddenly assess the vulnerability of regional bridges by adopting the latest Chinese seismic intensity standard and the instrumental intensity calculation method [35], as expressed in Eq. 1.

$$P[\mathrm{DS}_i \geq \mathrm{d}s_i|\mathrm{IM}_{\mathrm{CSIS}}] = \Phi\left(\frac{\ln(\mathrm{DS}) - \upsilon}{\chi}\right) = \frac{c_1}{\mathrm{DSi}} e^{\frac{-(\log(\mathrm{DSi}) - c_2)^2}{c_3}}, \quad (1)$$

where,

$P[\mathrm{DS}_i \geq \mathrm{d}s_i|\mathrm{IM}_{\mathrm{CSIS}}]$ is the probability that the bridge exceeds the specified vulnerability level ($DS_i \geq ds_i$) threshold under CSIS (intensity measure, *IM*). DS1, DS2, DS3, DS4, and DS5 are 1, 2, 3, 4, and 5, respectively. $\Phi[\bullet]$ is the optimized lognormal distribution function, and υ and χ are the mean and standard deviation of CSIS (IM). c_1, c_2, c_3 are the undetermined regression parameters of the updated model.

The vulnerability levels of 1409 SSGs, 107 CGs, and 612 ABs are evaluated, and the empirical vulnerability matrix of different macroseismic intensity zones (VII–X/XI zones) is established, as summarized in Table 3. It is worth emphasizing that the field reconnaissance team found that there are relatively few samples in the extremely seismic zone and that the damage features are similar. Therefore, the samples in zones X and XI are combined for vulnerability analysis in this study.

Taking FI as the quantitative parameter of fragility, the vulnerability comparison regression curve and the undetermined parameter matrix of the multidimensional prediction model are developed, as shown in Fig. 6 and Table 4. (a_n and b_n are the regression coefficients of ERM and GRM, respectively). To effectively achieve the actual vulnerability of bridge clusters in different intensity zones, a probability model (Eq. 2) for evaluating the actual cumulative damage of bridges (ACFP) is proposed by combining the risk and cumulative damage probability theory. An empirical vulnerability curve based on ACFP is developed, as reported in Fig. 7.

$$\mathrm{Vulnerability}_{\mathrm{bridges}} = P_{\mathrm{ACFP}}[\mathrm{DS}_i \geq \mathrm{d}s_i|\mathrm{IM}] \quad (2)$$

$P_{\mathrm{ACFP}}[\mathrm{DS}_i \geq \mathrm{d}s_i|\mathrm{IM}]$ is the cumulative failure probability of the actual bridge damage reaching or exceeding the *i*th damage level under a given *IM*.

Depending on the comparison of the vulnerability of the three types of bridges in different intensity zones, CG is slightly more damaged than SSG in zone VII, 73.2% of the samples are at the DS2 level, and AB is relatively more damaged. In zone VIII, the damage of the SSG and CG is slightly increased. It is worth noting that AB damage is further increased, and 1.5% of the samples have collapsed or local failure. In zone IX, the damage of the SSG is slightly lighter than that of the CG, and the damage of the AB is relatively severe. In zone X/XI, a small number of SSG samples are at the DS1 level, which indicates that this type of bridge has excellent seismic capacity, and the CG damage is significantly lighter than the AB damage. In terms of

Table 3 Empirical vulnerability probability matrix of typical bridges considering CSIS (Number/FI)

Bridge category	Seismic intensity	Vulnerability level					Total (number/failure index)
		DS1	DS2	DS3	DS4	DS5	
SSG	VII	299/0.394	424/0.559	36/0.047	0/0	0/0	759/1
	VIII	103/0.286	226/0.628	28/0.078	3/0.008	0/0	360/1
	IX	23/0.117	122/0.619	37/0.188	9/0.046	6/0.03	197/1
	X/XI	2/0.022	29/0.312	31/0.333	19/0.204	12/0.129	93/1
CG	VII	13/0.232	41/0.732	2/0.036	0/0	0/0	56/1
	VIII	5/0.192	17/0.654	4/0.154	0/0	0/0	26/1
	IX	1/0.071	7/0.5	5/0.358	1/0.071	0/0	14/1
	X/XI	0/0	1/0.091	6/0.545	2/0.182	2/0.182	11/1
AB	VII	105/0.379	133/0.48	37/0.134	2/0.007	0/0	277/1
	VIII	69/0.34	95/0.468	24/0.118	12/0.059	3/0.015	203/1
	IX	9/0.096	21/0.223	30/0.319	22/0.234	12/0.128	94/1
	X/XI	2/0.053	4/0.105	7/0.184	9/0.237	16/0.421	38/1

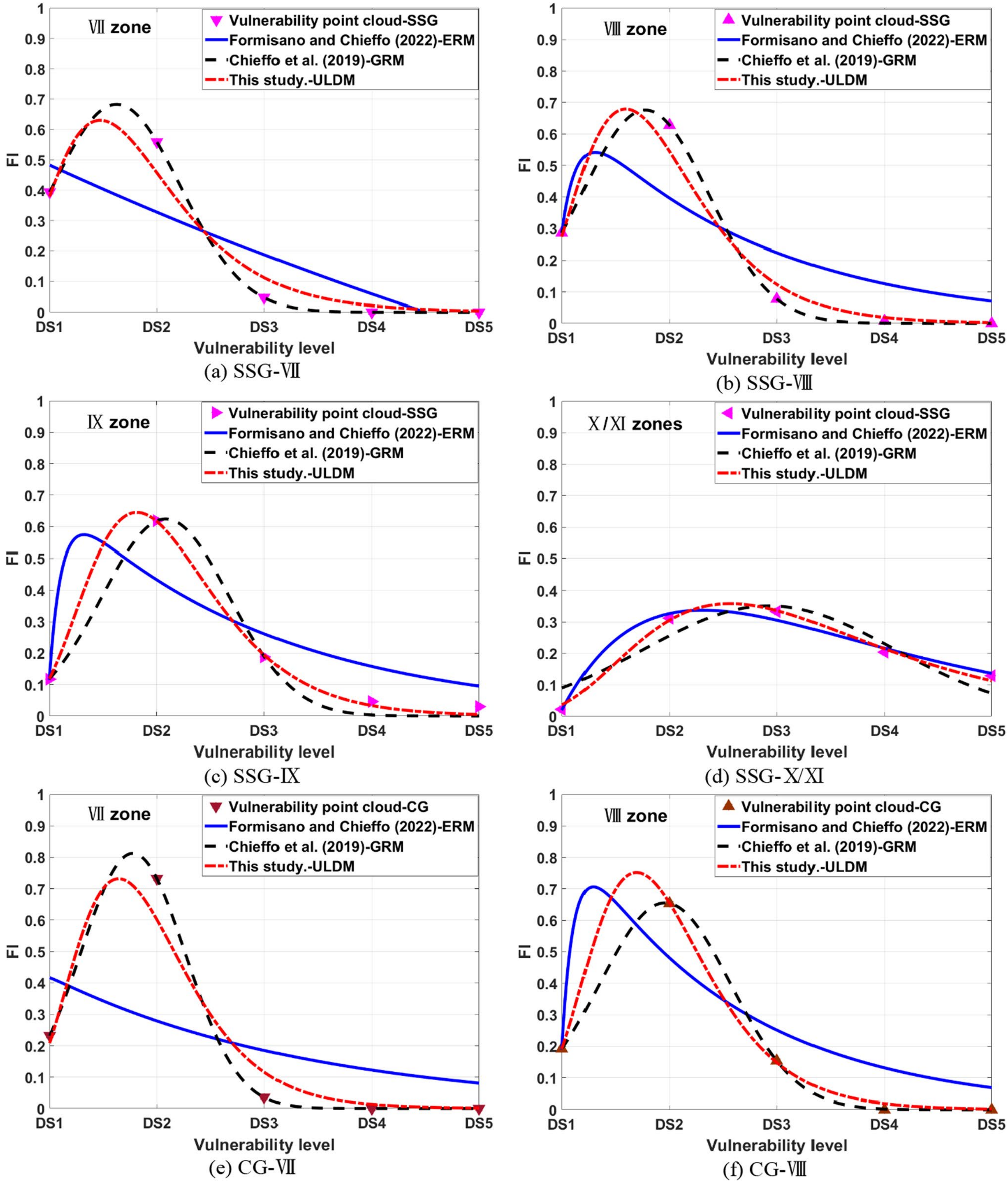

Fig. 6 Vulnerability regression curve of regional bridge clusters considering updating seismic intensity measure (CSIS/FI)

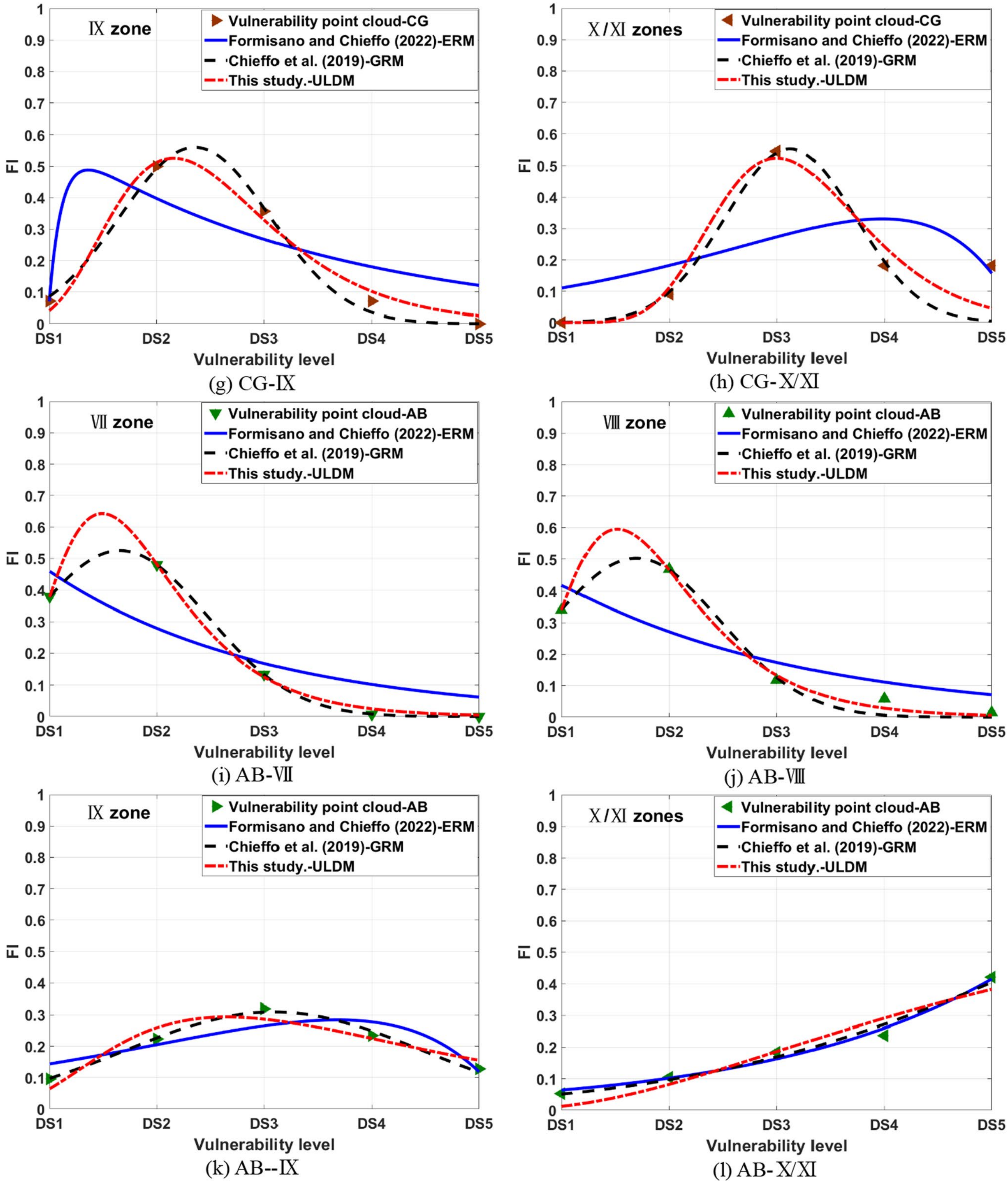

Fig. 6 (continued)

the vulnerability regression model, ULDM shows excellent robustness and regularity (the goodness of fit of all models is above 0.866). According to the comparison of three typical regression models, the damage of SSG and CG is similar, and the damage of AB is relatively heavy, which is highly consistent with the updated vulnerability matrix established

Table 4 Vulnerability regression parameter matrix of typical bridge clusters (FI)

Type	Seismic intensity	Vulnerability regression model										
		Formisano and Chieffo [33]				Chieffo et al. [34]			This study			
		ERM/a_n				GRM/b_n			ULDM/c_n			Goodness of fit
		a_1	a_2	a_3	a_4	b_1	b_2	b_3	c_1	c_2	c_3	
SSG	VII	2.484	– 0.083	– 1.831	– 0.015	0.683	1.624	0.841	0.998	0.533	0.294	0.944
	VIII	1.243	– 0.571	– 473.5	– 7.037	0.676	1.774	0.835	1.146	0.583	0.237	0.967
	IX	1.189	– 0.505	– 4005	– 8.805	0.625	2.084	0.84	1.235	0.702	0.21	0.996
	X/XI	– 3995	– 0.746	3994	– 0.745	0.351	2.928	1.653	1.012	1.135	0.387	0.991
CG	VII	0.635	– 0.411	– 27.17	– 8.779	0.813	1.776	0.693	1.263	0.595	0.197	0.938
	VIII	1.758	– 0.648	– 5188	– 8.873	0.656	1.959	0.865	1.338	0.627	0.202	0.999
	IX	0.879	– 0.397	– 2487	– 8.474	0.56	2.357	0.99	1.203	0.886	0.232	0.982
	X/XI	0.302	0.744	– 0.238	0.789	0.552	3.124	0.858	1.615	1.152	0.107	0.866
AB	VII	0.135	– 0.492	0.622	– 0.502	0.525	1.656	1.149	1.032	0.549	0.3	0.998
	VIII	0.658	– 0.443	– 384.9	– 11.45	0.503	1.693	1.113	0.975	0.572	0.311	0.992
	IX	423.8	0.619	– 423.7	0.619	0.309	3.087	1.944	0.912	1.29	0.629	0.871
	X/XI	– 0.144	0.47	0.184	0.469	0.895	9.461	5.006	9.823	3.188	1.523	0.919

and the field observations. In zone VII, the evaluation accuracy of ERM for SS, CG, and AB is significantly weaker than that of GRM and ULDM. In zone VIII, the GRM of SSG is better than the goodness of fit of ERM, but there is the possibility of overfitting. The ULDM curve of CG is closer to the actual seismic damage characteristics of bridges compared to the other two models. In zone IX, the ERM evaluation of SSG and CG is relatively light, and the GRM is relatively heavy. The goodness of fit of the ULDM curve reaches 0.996 and 0.982. In zones X/XI, the similarity of the three regression models for SSG and AB is relatively high, and the prediction accuracy of ULDM and GRM for CG is slightly higher than that of ERM. Depending on the ACFP curve, the difference in the damage of the three bridges in zones VII and VIII is relatively small. Starting from zone IX, the damage of the three bridges is significantly increased, and the ACFP curve increases rapidly in DS4 and DS5 levels. The damage of AB in different intensity zones is relatively serious, so it should be considered to reasonably improve the seismic capacity of this type of bridge.

4 Comparison of bridge vulnerabilities under the influence of single factors

4.1 Premise

The traditional seismic vulnerability analysis of bridges employs different methods to establish the relationship model between intensity measures and engineering demand parameters to obtain the failure modes of bridges under varying levels of ground motion [36]. However, from the on-site investigation of the seismic damage of bridges and the data collected and processed from the investigation database, it was found that the level of bridge vulnerability depends significantly on the bridge length, coordinate azimuth of the bridge site, number of spans, cross-sectional form of the piers, types of bearings and foundation, and linear design-influencing factors. The different influencing factors have direct effects on the typical bridges in the corresponding seismic regions and cause the different types of bridges to suffer different degrees of damage. This study innovatively proposes a correlation assessment analysis method between the macroseismic failure level and actual cumulative failure probability under the influence of multiple bridge characteristic factors. This method develops a new model for the actual earthquake fragility assessment of typical bridges with different bridge characteristic dimensions.

To explore how each factor influences bridge vulnerability, this paper considers each of the above influencing factors and makes a comparative analysis of the empirical vulnerability of SSG, CG, and AB to earthquake damage. When researching each of the above factors, the parameter independence and noncorrelation method is used to control the influence of other factors. By comparing the damage differences among them, the novel vulnerability model of the different bridge types is established based on the specific influencing factors, thereby providing a necessary allusion for promoting and improving the seismic performance of typical bridge structures.

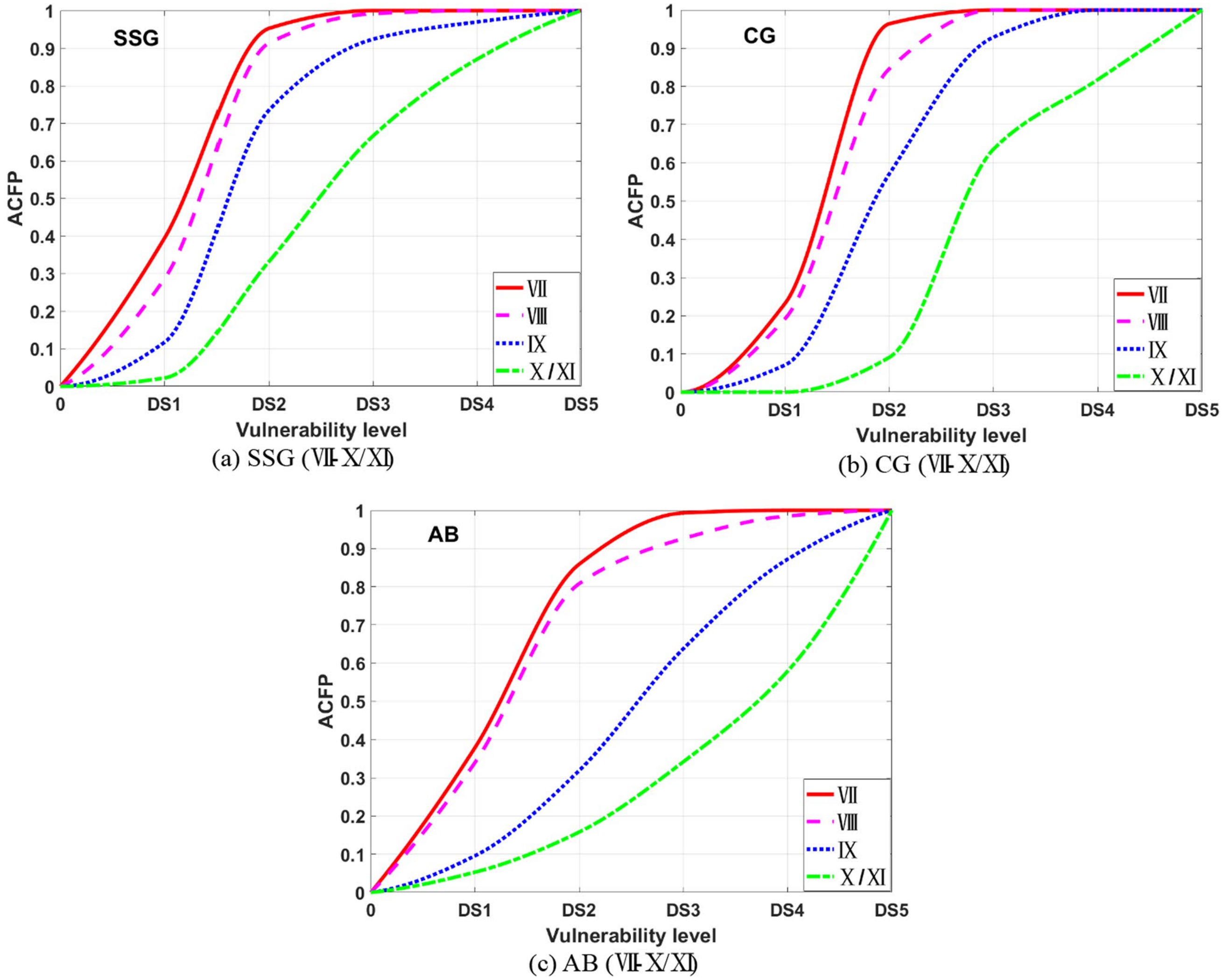

Fig. 7 Vulnerability curve of regional bridge clusters considering updating seismic intensity measure (CSIS/ACFP)

4.2 Bridge length (BL)

Because of the functional requirements of a bridge, its length should be designed according to the actual site conditions. Therefore, SSG, CG, and AB with different BLs show significant failure characteristics under the action of ground motion. To study the fragility of typical bridges under the influence of different BL factors, the bulk of statistics and induction are made on SSG, CG and AB, and the vulnerability survey sample (VSS) distribution based on the BL factor is drawn. Combined with the nonlinear vulnerability model and the principle of regression analysis [37], the updated nonlinear model (Eq. 6, Gauss quadratic fitting model (GQFM)) was used to perform regression analysis on the sample points. The SSG, CG, and AB regression comparison fragility curves were obtained based on the empirical seismic-damage database. The field observation sample data of three types of typical bridges are counted according to the BL factor, the statistical vulnerability matrix based on BL is established, and the vulnerability point cloud, plane, surface and curves of typical bridges are generated by using two-dimensional and three-dimensional numerical modal calculation methods and updated nonlinear regression models, as shown in Fig. 8.

According to the statistics of the actual bridge sample data and the analysis of the point cloud, plane, surface and nonlinear regression model (GQFM), the damage of SSG, CG, and AB is relatively light when the BL is short. The BL factor has the most significant effect on AB vulnerability, with AB damage being relatively heavy between DS2 and DS3. According to regression analysis, the maximum BL for AB is ~ 425 m. CG is obviously affected by BL at the DS2 level, with BL reaching a maximum at ~ 250 m. The influence of BL on the overall sample distribution and regression model of SSG is not obvious. At the DS2 level, the damage

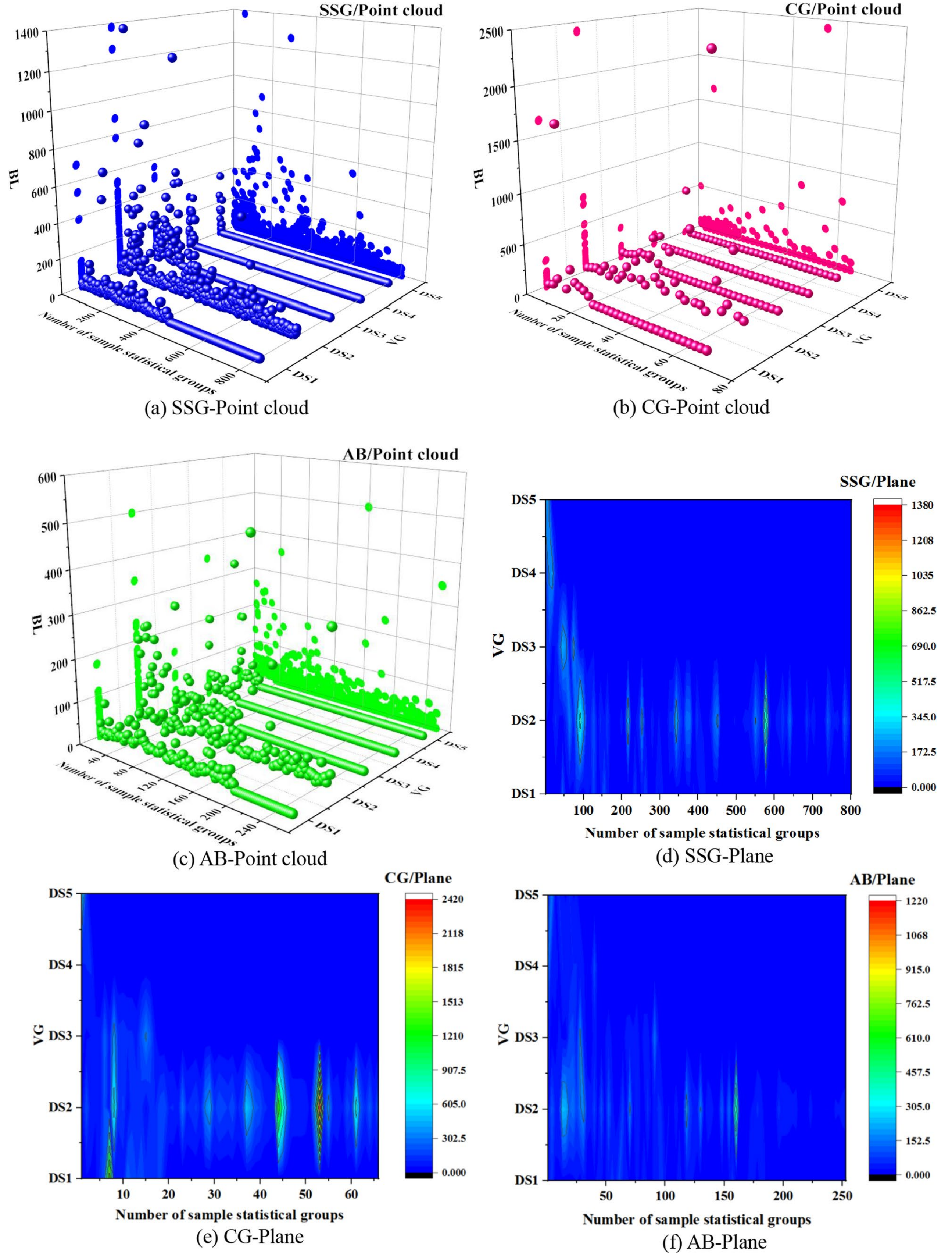

Fig. 8 Comparison of vulnerabilities models of typical bridges based on bridge length (BL/m) factor

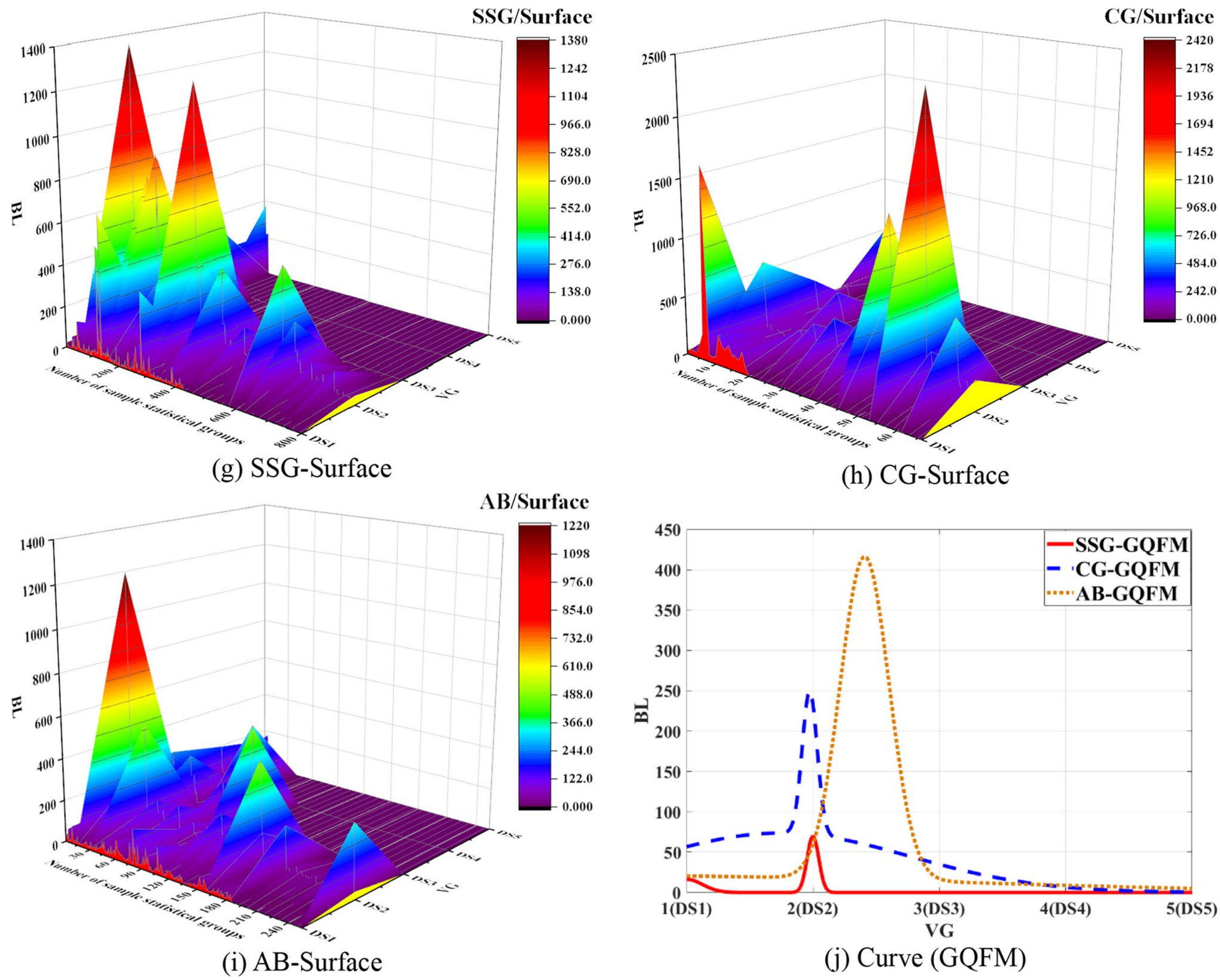

Fig. 8 (continued)

limit is reached at ~ 70 m. Considering the BL influencing factor, the overall failure of the three typical bridge types is relatively prominent in DS2–DS3. The design lengths of different bridge types should be controlled reasonably in the design of BL, which should be controlled and designed effectively in the case of considering the damage of different vulnerability levels.

4.3 Coordinate azimuth (CA) of bridge site

In the investigation, it was found that the CA at different bridge sites had a certain impact on the bridge damage; the direction of bridge construction differed, and the damage to the different types of bridges was obviously different. Therefore, we selected some typical information about the bridge construction sites and collected a large amount of CA data combined with statistical theory and nonlinear model regression to study the fragility of various typical bridges under the influence of the CA factor, and the statistical fragility matrix of three groups of bridges was established. Using multidimensional numerical modal calculation means and an updated regression model analysis method, three types of bridge fragility comparison point clouds, planes, surfaces, and curves based on the CA influencing factor are developed, as shown in Fig. 9.

According to the results of classifying and analyzing the sample data according to CA, for SSG, it is noticeably that there were fewer damaged samples at the DS2 level, and the distribution of bridge samples was relatively concentrated between 120 and 230–350° at the DS3 level. For CG, the influence of CA was reflected mainly in the DS3 and DS4 grades, with relatively concentrated failure at 30°, 50°, and 250°. For AB, DS2 was relatively large in the ranges of 80–100°, and 70–90°. The sample size of DS3 is approximately 150° of CA, and the sample sizes of DS4 and DS5 are large at 50° and within. According to the vulnerability

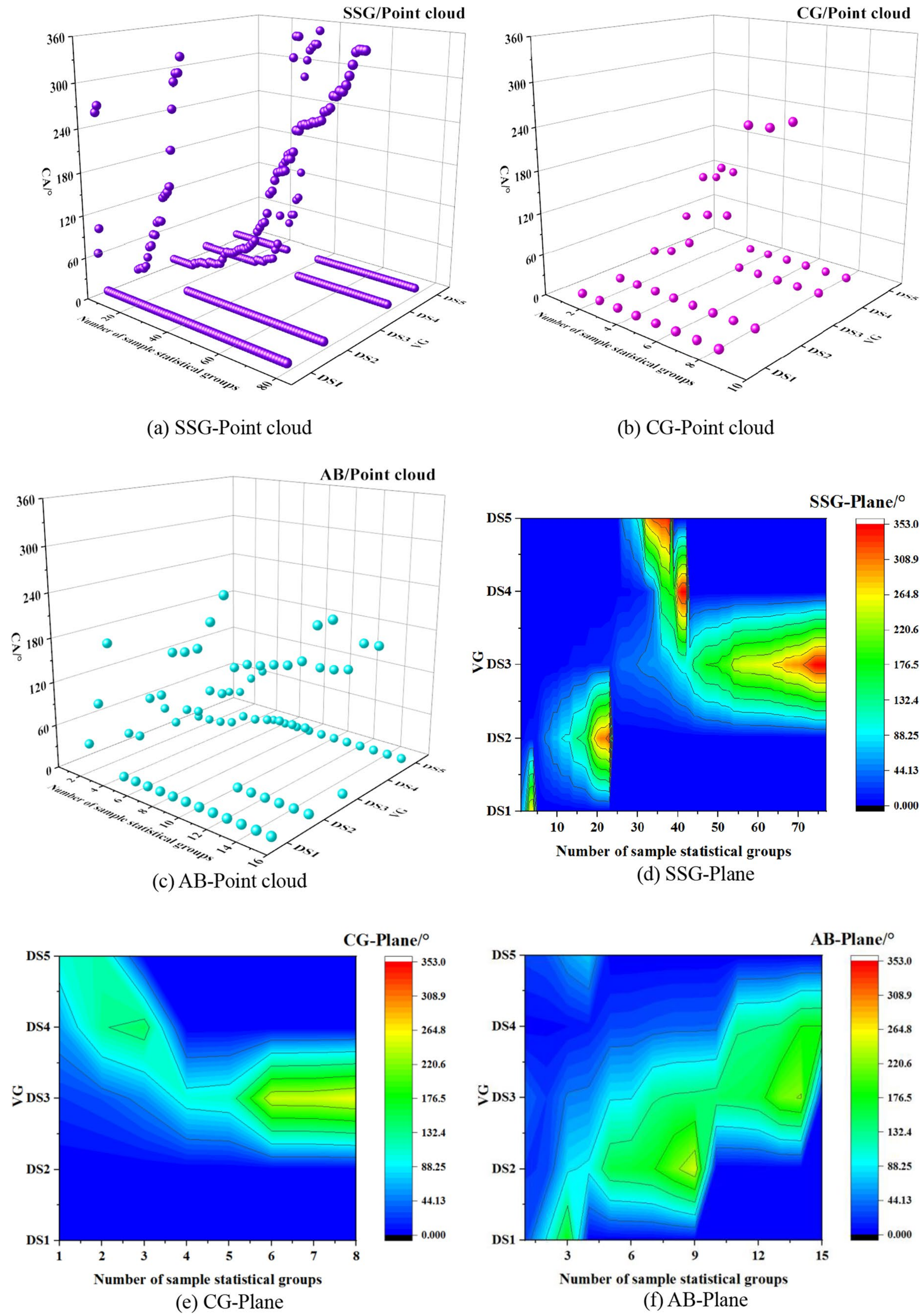

Fig. 9 Comparison of vulnerability models of typical bridges based on coordinate azimuth (CA/°) factor

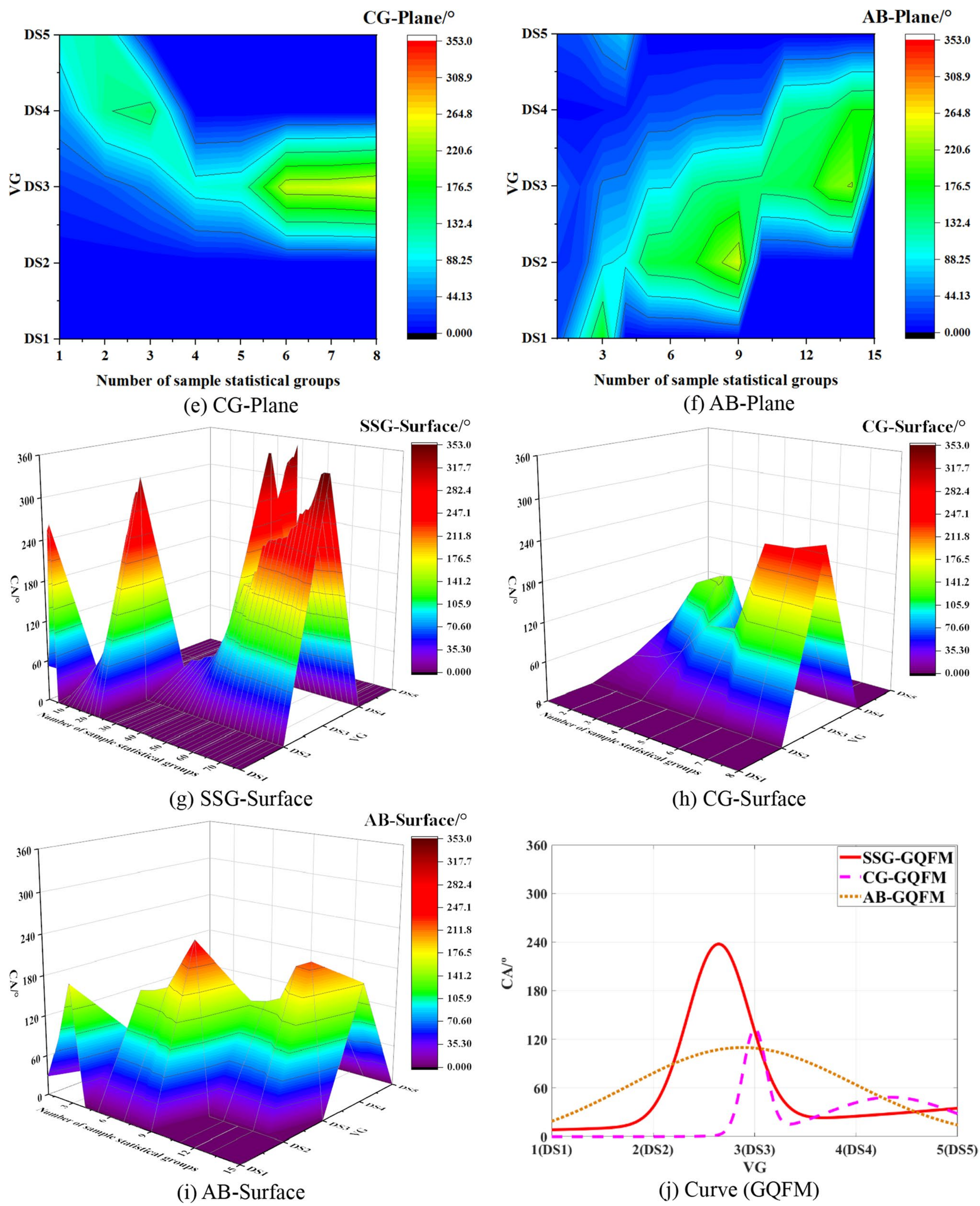

Fig. 9 (continued)

regression model, CA has a great influence on the number of DS2 and DS3 grades of each structure type, which should be taken into account as one of the reference indexes for bridge site selection.

4.4 Span (S)

A large amount of historical seismic observation data indicates that the span has a very significant impact on bridge vulnerability, and a detailed study of the S factor of typical bridges can effectively guide the assessment of the seismic damage of bridges. From the seismic-damage observation data, consideration was given to the number and length of different spans ($m \times n$, where m is the number of spans and n is their length) and the vulnerability situation in the actual seismic damage, leading to statistics for the SSG, CG, and AB data.

The traditional cumulative failure-exceedance probability parameter is the essential index to virtually evaluate the vulnerability of typical regional bridges and buildings [38]. This study adequately considers the failure probability parameter features of actual bridge clusters, updates the logarithmic probability distribution density function model (Eq. 1), and proposes a new logarithmic distribution function for vulnerability assessment based on actual cumulative failure-exceedance probability (ACFP) and bridge characteristic parameters, as expressed in Eq. 3.

$$P(\mathrm{DS} \geq \mathrm{DS}_i \,\big|\, \mathrm{BCP}_j) = P(p_{\mathrm{ACFP}} \geq p_i), \tag{3}$$

where BCP_j is the *j-th* bridge characteristic parameter (including the single and coupling factors mentioned in this

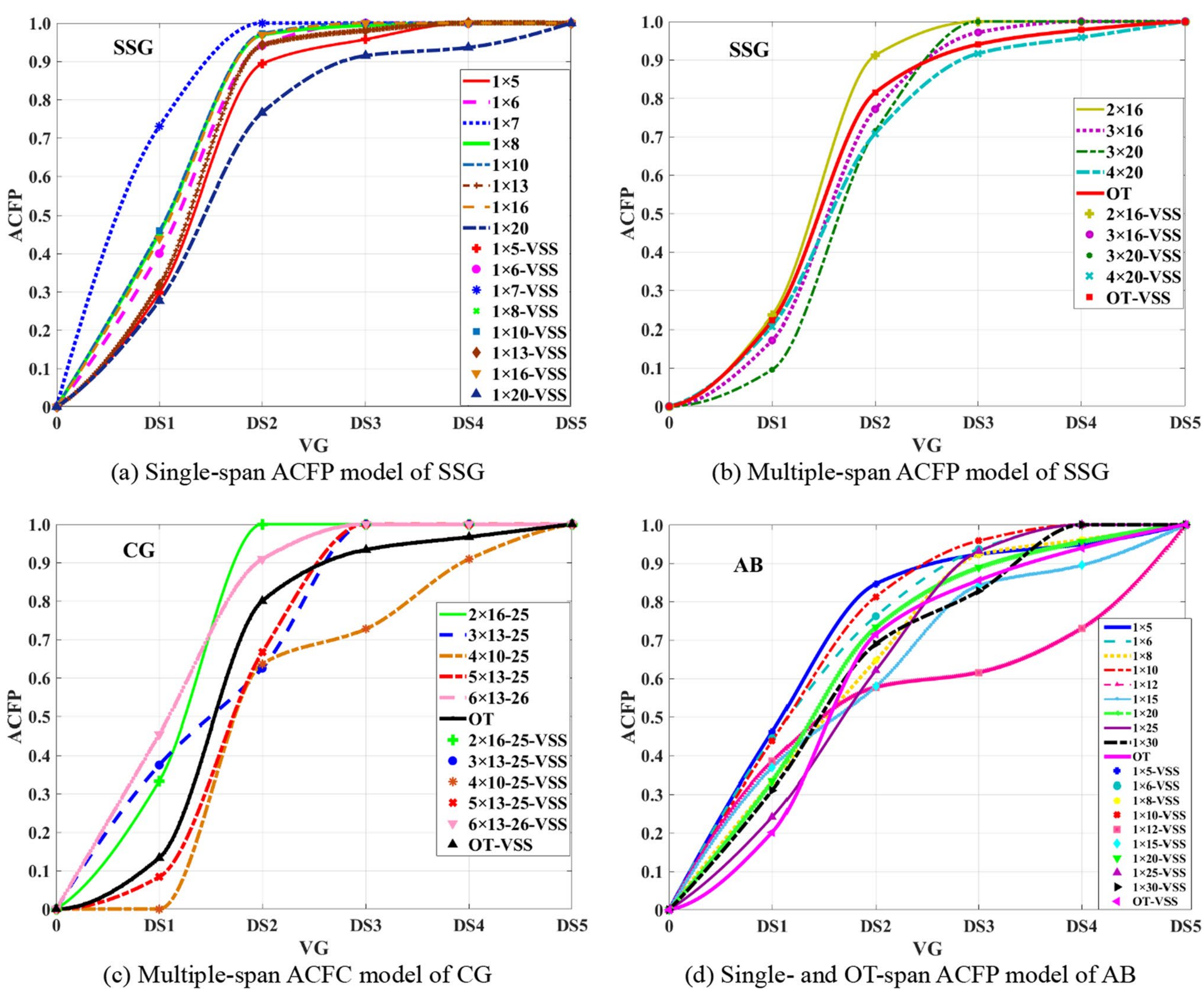

Fig. 10 Comparison of single-span and multiple-span vulnerability models of typical bridges

study), $P(\bullet)$ represents the logarithmic distribution function of the ACFP based on different vulnerability levels, and p_i is the actual failure probability of the *i-th* vulnerability level ($i = 1, 2, 3, 4, 5$).

Combining a traditional cumulative probability distribution function and numerical analysis, the novel ACFP model curves of the vulnerability of the three types of typical bridges with different span numbers and lengths were drawn, as shown in Fig. 10.

The damage to SSG bridges (single-span) is relatively prominent. From analyzing the ACFP model, the damage of bridges (single-span) with a span of 7 m is lighter, that of those with a span of 20 m is the most severe, and that of bridges with a span of 5 m is more severe than that of those with spans of 6, 8, 10, 13, and 16 m. The damage of 2 × 16-m multi-span bridges is relatively light, while the damage of 4 × 20-m SSG is relatively heavy, but the difference is not significant. The other mixed-span SSG vulnerability models are in the middle of the comparison curves, and the conclusions of the model are consistent with the empirical seismic damage observations. The length and quantity of single-span and multi-span bridges can be set reasonably by combining model analysis. CG bridges commonly have many spans and links. According to the analysis of the ACFP model, the damage of the 4 × 10–25-m CG bridges is relatively heavy, that of the 2 × 16–25-m CG bridges is relatively light, and the number of spans of the whole CG sample has a relatively significant impact on the vulnerability. It is necessary to reasonably control the number of spans of CG bridges and to use the method of setting expansion joints to increase the ductility of the structure to improve its seismic level. AB bridges mainly have one span. According to the analysis results of the ACFP model, the damage of 1 × 12 m is relatively heavy. Compared with the one-span SSG bridge, the seismic damage is more serious, so the overall design of AB bridges should be improved to ensure that AB bridges of various materials have a certain lateral dynamic load resistance.

4.5 Pier type (PT)

The different geometric types of pier columns suffered different seismic damage in areas of different intensities. Therefore, it is of practical significance to consider how pier geometry influences the vulnerability of typical bridges. There were various types of piers in the Wenchuan earthquake area, including bent piers (P1), single-column piers (P2), rectangular thin-walled piers (P3), masonry entity piers (P4), composite piers (P5), other piers (P6), and single span without piers (N/A). The empirical seismic-damage survey samples were classified and counted according to the geometric type of pier columns, the vulnerability analysis was conducted by using the ACFP model, and the vulnerability model comparison curves of SSG, CG, and AB under the influence of different geometric form factors of pier columns were drawn as shown in Fig. 11.

The vulnerability of SSGs with different geometry types is not significant. N/A damage was relatively light, P3 damage was relatively heavy, P1 was slightly heavier than P4, and P4 damage was slightly heavier than P2. Among the various types of piers selected for CG, P2 was relatively damaged, P3 was relatively light, and P1 was slightly heavier than P4. The damage of P1 and P3 in AB was similar and slightly lighter than that of N/A and P4, and that of N/A was slightly lighter than that of P4. When P1 is selected for the three types of typical bridge piers, the damage of AB was relatively light, and CG was slightly lighter than SSG. To some extent, this indicates that it would be reasonable to use P1 in AB and CG bridges. For the P2 type, the failure of SSG was relatively light, while CG was relatively heavy; therefore, it would be reasonable to use P2-type piers in SSG bridges. For the P3 type, the damage of CG was relatively light, while SSG was relatively heavy, and AB was slightly heavier than CG; therefore, it would be reasonable to increase the proportion of AB's DS1 grade and improve its seismic capacity in accordance with the requirements of the seismic design code (JTG/T 2231-01, China) [28]. For the P4 type, the overall damage of CG was relatively light, but the number of DS1 grades was scarce, and the damage of AB was obviously heavy; therefore, it is necessary to restrict the use of this type of pier or increase structural measures to improve its seismic capacity. In the case of N/A, the damage of SSG was significantly lighter than that of AB, which suggests that the SSG bridges without piers have better seismic capacity, and the probability of exceeding DS2 is less than 5%, basically achieving the seismic design goal of Chinese bridges.

4.6 Foundation type (FT)

The selection of bridge foundation type is related directly to the site conditions, and the empirical seismic-damage survey data showed an obvious difference in the damage of different types of typical bridges. To analyze the vulnerability characteristics of bridges with different foundation types, the empirical seismic-damage survey database was processed statistically. The foundation types in the Wenchuan earthquake survey area were commonly one of three categories: expansion foundation (F1), pile foundation (F2), or mixed foundation (F1 + F2). Combined with the ACFP model, a comparative vulnerability analysis based on the FT factor was conducted for the different foundation and bridge types, and the vulnerability model curves were drawn, as shown in Fig. 12.

According to the analysis results, for the F1 type, the damage of SSG was significantly lighter than that of AB,

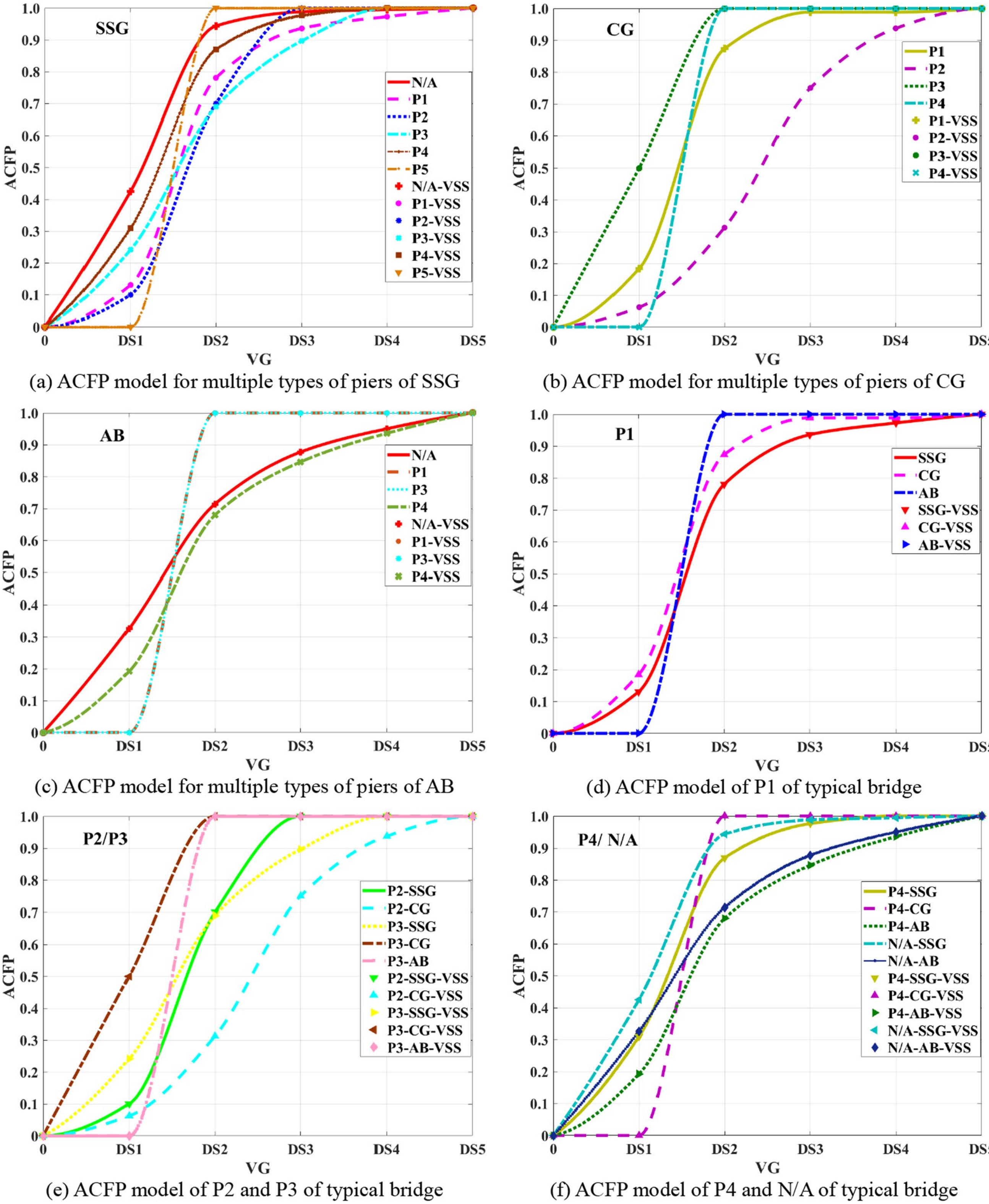

(a) ACFP model for multiple types of piers of SSG

(b) ACFP model for multiple types of piers of CG

(c) ACFP model for multiple types of piers of AB

(d) ACFP model of P1 of typical bridge

(e) ACFP model of P2 and P3 of typical bridge

(f) ACFP model of P4 and N/A of typical bridge

Fig. 11 Comparison of vulnerabilities of typical bridges based on geometric type (PT) factor

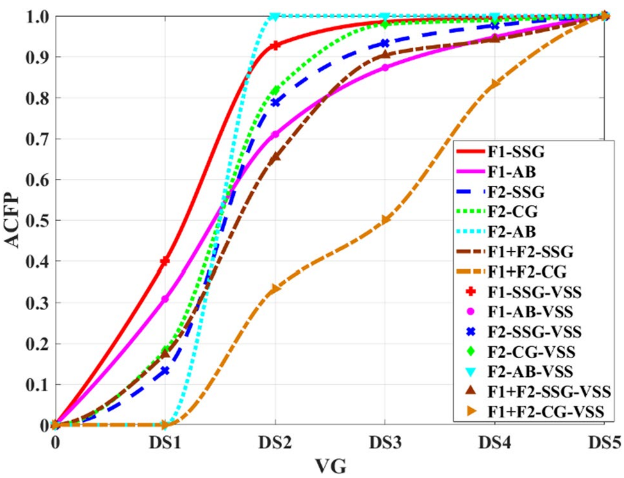

Fig. 12 Comparison of vulnerabilities of typical bridges based on foundation type (FT) factor

and most of the SSG occurrence probability was at the DS1 and DS2 levels. For the F2 type, there was no remarkable discrepancy among the three types of typical bridge damage, CG was slightly heavier than SSG, and AB sample damage occurred at the DS2 level, slightly lighter than for SSG and AB. For the F1 + F2 type, the damage of CG was more serious than that of SSG, and the damage of this mixed foundation was more serious than that of typical bridges using F1 or F2 alone. Therefore, it would be reasonable to select the F1 and F2 types and use F1 + F2 cautiously, and necessary anti-seismic measures should be taken to reduce the probability of occurrence of higher vulnerability levels and improve the probability of DS1 grade occurrence to improve the earthquake capacity of various typical structures from the selection of foundation type.

4.7 Bearing type (BT)

The bearings of a bridge are important components and play an essential role in determining its overall seismic capacity. However, there are some apparent anomalies in the seismic damage of different bearing types. To study how the bearing type affects the vulnerability of typical bridges under seismic action, the SSG, CG, and AB samples from the actual Wenchuan earthquake damage investigation were classified and counted. The main bearing types were laminated rubber bearings (B1), basin rubber bearings (B2), other bearings (B3), and no bearings (B4). The ACFP model was still applied to the regression and failure analysis of SSG, CG, and AB under different bearing types, and typical bridge-vulnerability comparison curves based on the BT factor were drawn, as shown in Fig. 13.

According to the data analysis results, the failure modes of SSG and CG were relatively similar to those of the B1 type, and AB was slightly lighter. Regarding B2, the damage of DS1 and DS2 of the SSG was inconspicuous, and the survey data indicated that there were no samples of this type of bearing at the DS2 level, so the curve model was abnormal. B3 is commonly used in various bearing forms, and the difference between SSG and AB is implicit, with the former being slightly heavier than the latter. B4 is common for bridges with small spans, for which no bearings are set, so the damage of this type of bridge was relatively prominent. The damage data and probability curve show that SSG was significantly lighter than AB. The BT factor has a direct impact on bridge vulnerability. In the investigation, many bearings had been damaged, resulting

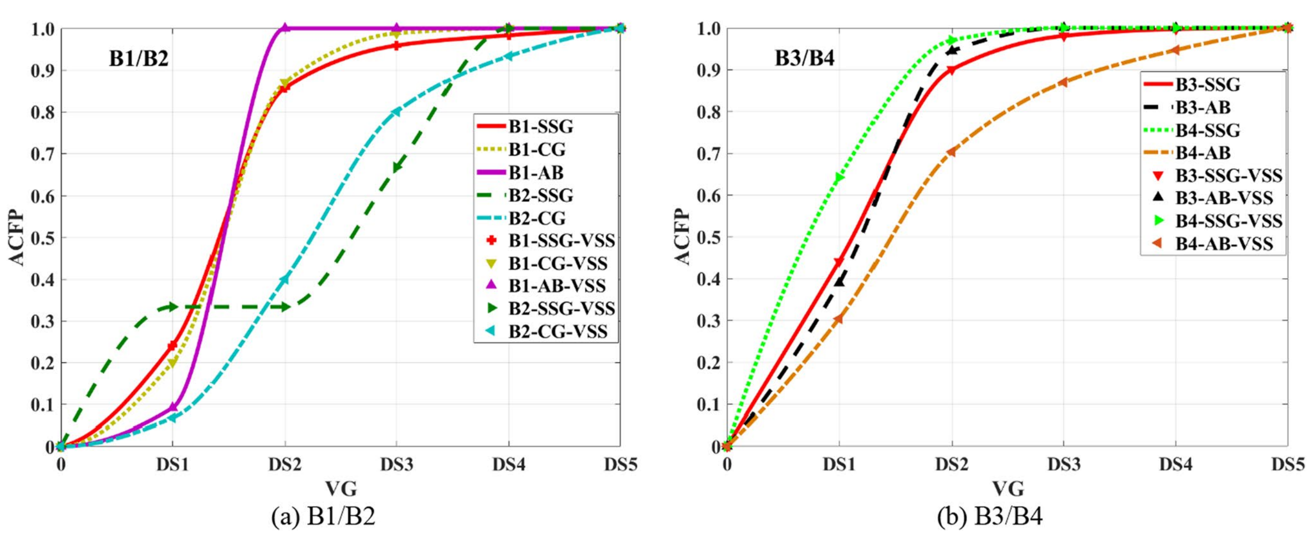

Fig. 13 Comparison of vulnerabilities of typical bridges based on bearing type (BT) factor

in either serious damage or partial or even total collapse of the bridge. In addition to ensuring the requirements of the bearings themselves, it is also necessary to (i) select the appropriate bearing type, (ii) strengthen the lateral force resistance of the bearings and their connections with the upper and lower structures, and (iii) improve the integrity and ductility of the bridge.

5 Comparison of bridge vulnerabilities under influences of coupled factors

5.1 Premise

According to the empirical seismic-damage reconnaissance data and field investigation of typical bridges, in addition to bridge vulnerability being influenced by single factors, the influence of coupled factors affects bridge damage to a certain extent. Therefore, it is necessary to analyze the vulnerability and seismic performance of typical bridges under the influence of coupled factors to provide a scientific reference for the future seismic design of typical bridges.

5.2 Coupling of linear type (L) and BL

The main types of bridges in earthquake areas are straight-line (SL) and curved-line (CL) ones, and according to the investigation, different types of typical bridges with different line types and bridge lengths were damaged to different degrees. Under the influence of SL and CL coupling factors, SSG, CG, and AB all showed significant vulnerability differences. To study the fragility characteristics of each typical bridge under the influence of coupled factors, the sample database was evaluated according to the line type and length of the different types of bridges, and the statistics were summarized. To ensure the goodness of fit of the nonlinear vulnerability regression model, we updated and refined the original Gaussian model [39] and proposed a Gaussian mixture order fitting model (Gaussian first-fit model (GFFM) and GQFM). Depending on the multidimensional numerical mode and cloud analysis theory, SSG, CG, and AB vulnerabilities were compared, and comparative point cloud, plane, surface, and updated failure curves considering L and BL coupling factors are drawn in Fig. 14.

The empirical seismic-damage survey samples and the model regression show that the damage of each typical SL bridge exhibits apparent anomalies. The damage grades of SSG, CG, and AB are all concentrated in DS2. In SSG, BL reaches the maximum value of seismic damage between 50 and 100 m, while the damage of the other vulnerability grades is inconspicuous. Meanwhile, CG reaches the peak value at 250 m, and the high probabilities of damage are concentrated in DS2. The fitting model of AB is relatively stable, with a small peak in DS2. BL is similar to SSG, and the other vulnerability levels are relatively balanced. In terms of CL, the peak value of SSG occurs between 50 and 100 m of BL and at the DS2 level, and then a small peak appears around DS3; meanwhile, BL is ~ 25 m. In CG, the peak value occurs at BL close to 150 m, and the location is between DS2 and DS3. In AB, the peak size is similar to that in SSG, but the damage degree is heavier than that in SSG, and the majority of the damage probability occurs in the interval of DS2 and DS3.

Different bridge types differ greatly in their damage situation under the coupled effect of L and BL. Therefore, it is necessary to (i) improve the seismic capacity of specific bridge types whose vulnerability level is prone to a damage peak, (ii) avoid any damage due to selecting a dangerous BL value and linear type, and (iii) take necessary measures to improve the weak vulnerability level and the seismic capacity of BL so that all types of bridges can be improved.

5.3 Coupling of PT and FT

The pier columns and foundation are important components of bridge substructures, and the damage in the Wenchuan earthquake was also relatively typical [40]. The difference between PT and FT directly affects the vulnerability of all types of typical bridges. To explore the seismic damage of bridges under the coupled action of these two types of single factors, the sample database was classified and summarized. Then, combined with the ACFP model and numerical analysis, a comparative analysis of vulnerabilities under the influence of the coupled PT and FT factors was conducted, and vulnerability analysis curves were drawn, as presented in Fig. 15.

According to the influence of the coupled PT and FT factors and the analysis of the ACFP model, with the F1 foundation type, the damage of the N/A type of AB is obviously heavier than P4, the P1 form of SSG is heavier than P3, P4 is similar to P3 damage, and N/A damage is relatively light. For the F1 foundation type, priority should be given to SSG with a short span and no pier columns; if the span is large, the P4 type of pier column should be considered. With the F2 foundation type, the damage of P1 and P4 is similar to that of AB. The probability of vulnerability exceeds the probability, and the probability of occurrence is at the DS2 level. The CG damage with the P1 pier type is obviously less than that with P2, while SSG with P1 columns is slightly heavier than that of CG. In the case of the F2 type, CG should give priority to the P1 type pier.

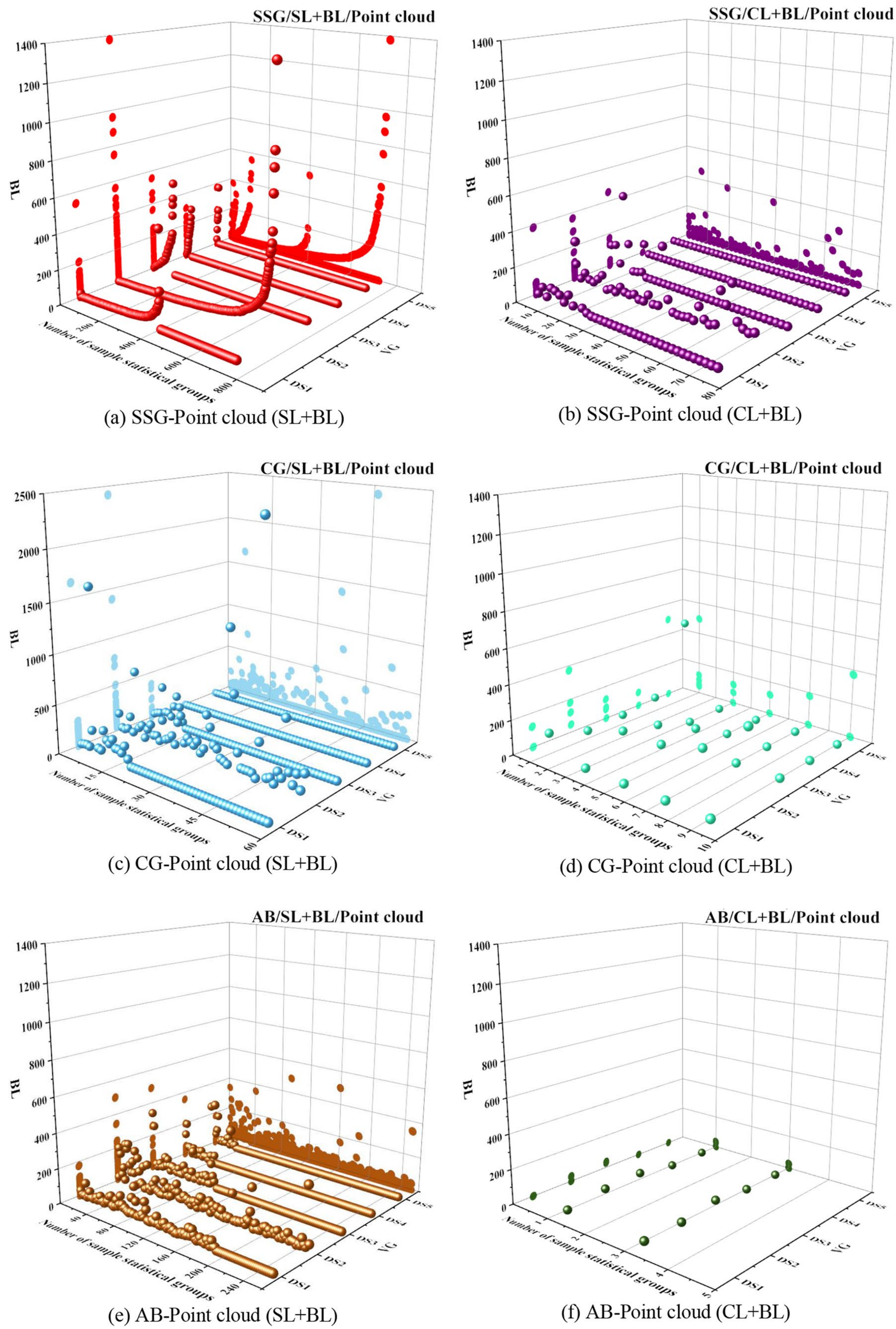

Fig. 14 Comparison of vulnerability models of typical bridges based on coupled L and BL/m factor

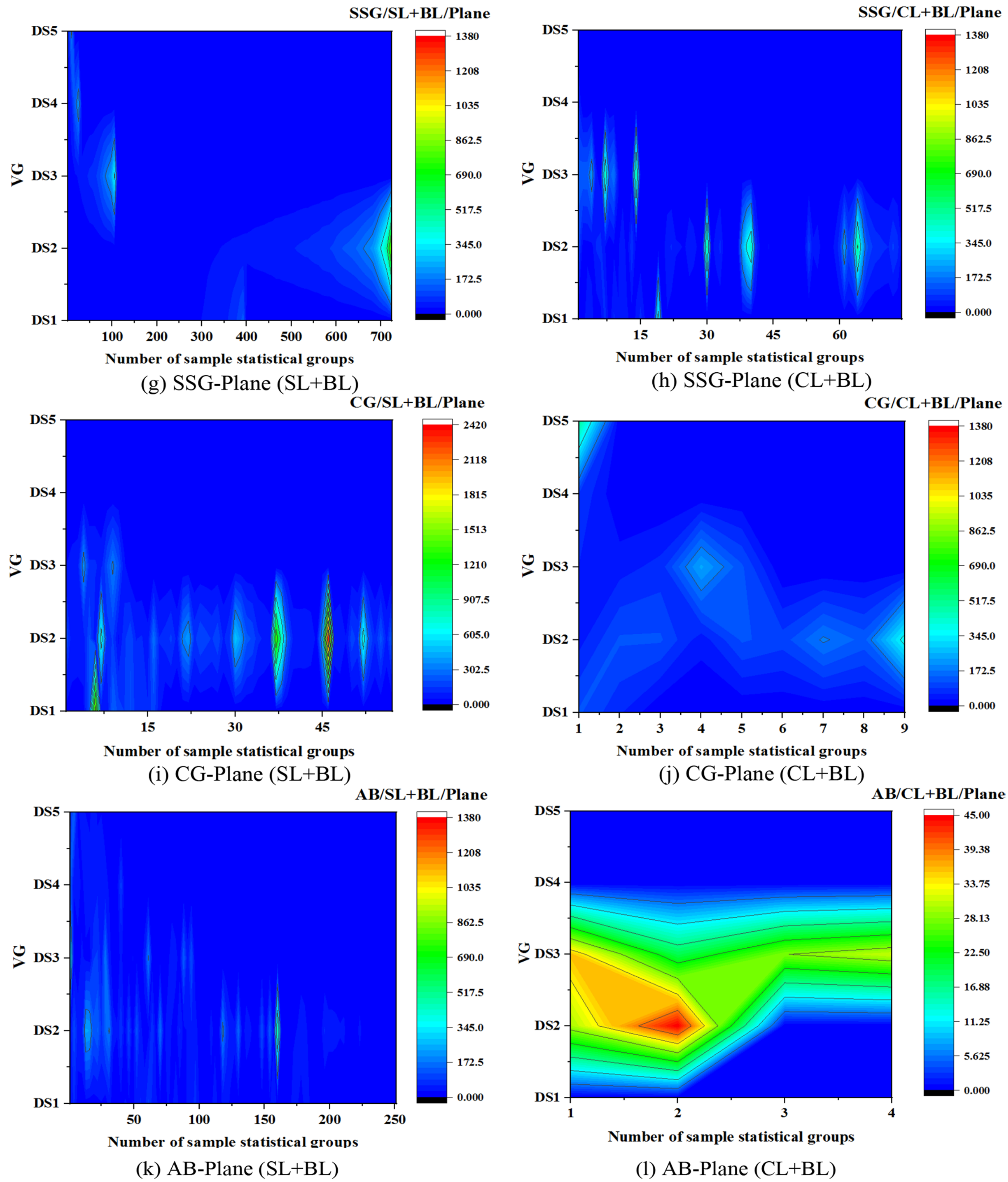

Fig. 14 (continued)

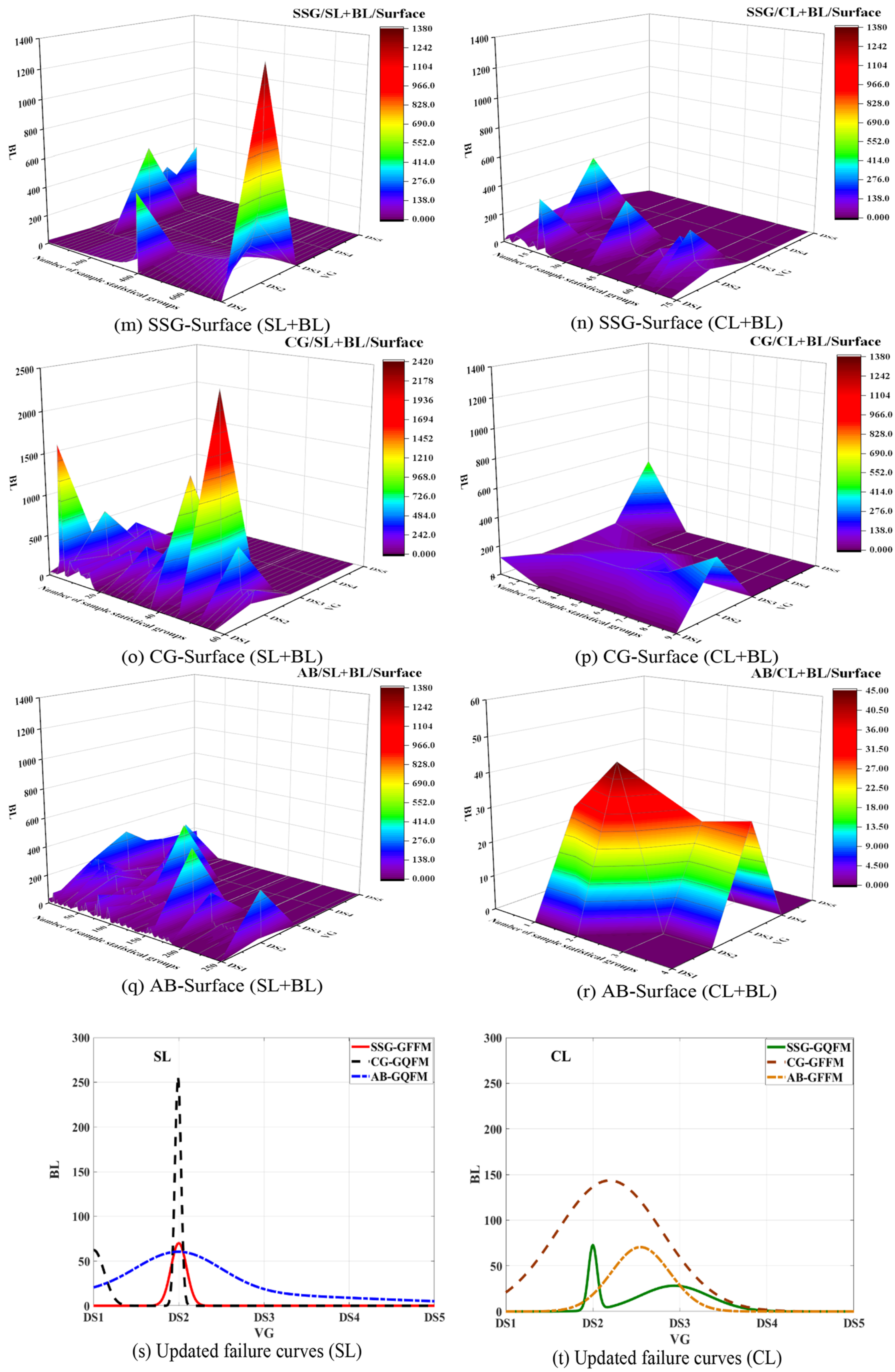

Fig. 14 (continued)

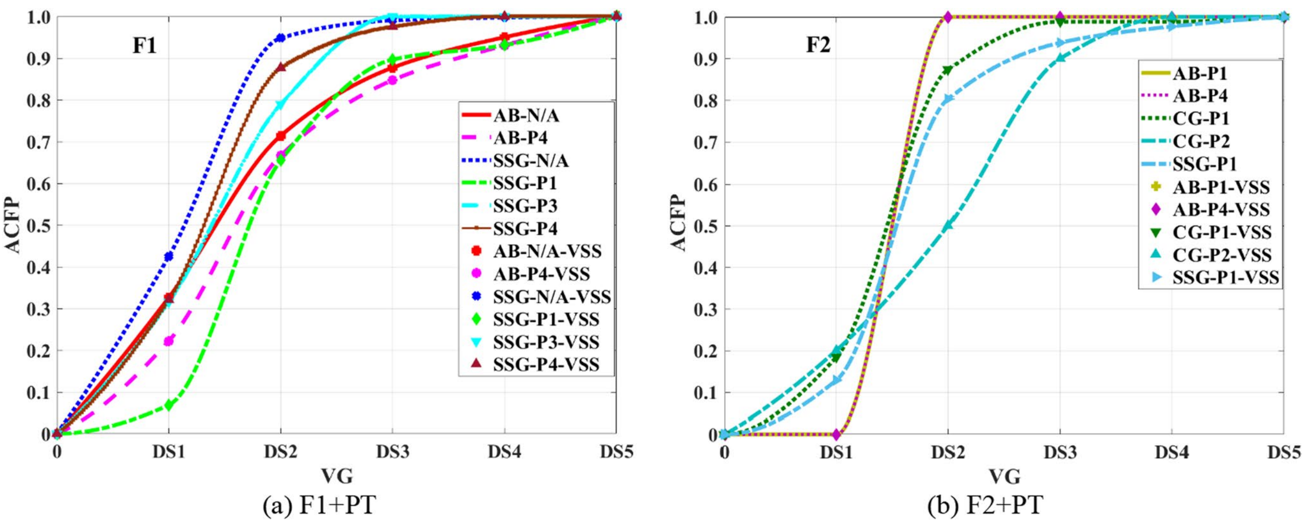

Fig. 15 Comparison of vulnerabilities of typical bridges based on coupled PT and FT factors

5.4 Coupling of FT, L, S, and BT

According to the field investigation and data collation of bridge damage, the difference between typical bridges under the influence of multifactor coupling is relatively significant. This study conducted the coupling field analysis of AB, SSG, and CG according to the FT, L, S, and BT. The sample data of the actual seismic damage bridge were deeply summarized, and the sample data without representative samples were eliminated. Using the ACFP model and vulnerability regression analysis method, a bridge vulnerability comparison model based on AB, SSG, and CG under multifield coupling was established, as depicted in Fig. 16.

In the single-span straight-line bridges with F1 and B4, the seismic damage of SSG is significantly lighter than that of AB, and the earthquake loss of bridges is similar to that of B1 and B3. Under the influence of multifactor coupling, the earthquake loss of the AB curve bridge is relatively heavy, and the correlation between the vulnerability of the SSG with F1 and the type of support is low. The analysis results indicate that an SSG with a small span should be prioritized in selecting a single-span bridge. The multifactor coupling multispan bridge adopts B3, the seismic damage is relatively light, and the exceedance probability is more than 0.7 at the DS2 level. The CG with B2 has significant seismic damage, and a greater likelihood occurs in DS3 and DS4. It should be considered to prioritize promoting the selection of B1 and F2 for multispan bridges and avoid selecting B2 in CG seismic design.

6 Conclusions

Typical bridge structures (simply supported girder bridges (SSGs), continuous girder bridges (CGs), and arch bridges (ABs)) were processed statistically based on sample data from an empirical bridge-damage investigation after the Wenchuan earthquake. Combined with criteria for evaluating the vulnerability level, two-dimensional and three-dimensional numerical moire model calculation methods, the empirical seismic-damage vulnerability statistical matrix, plane, point cloud, surface and curve model considering failure index and actual cumulative failure-exceedance probability (ACFP) were established, and a comparative analysis was performed.

Using the latest version of the Chinese seismic intensity standard (CSIS), a polymorphic vulnerability comparison model of typical bridge clusters considering different intensity zones is developed. On the basis of the traditional lognormal distribution, an updated normal lognormal distribution model considering CSIS is developed, and the rationality of the model is verified by using 2128 bridge samples that were hit by the Wenchuan earthquake. The ULDM analysis results indicate that the goodness of fit of various bridge damages is above 0.866, which verifies the rationality of the model.

This study breaks through the traditional evaluation mode of bridge vulnerability and innovatively proposes a correlation model analysis method between the macroseismic failure grade (vulnerability level) and actual cumulative failure probability under the influence of multiple bridge characteristic factors. Based on bridge length, coordinate azimuth, span, pier type, and foundation type and according to the vulnerabilities of SSG, CG, and AB under the bearing type

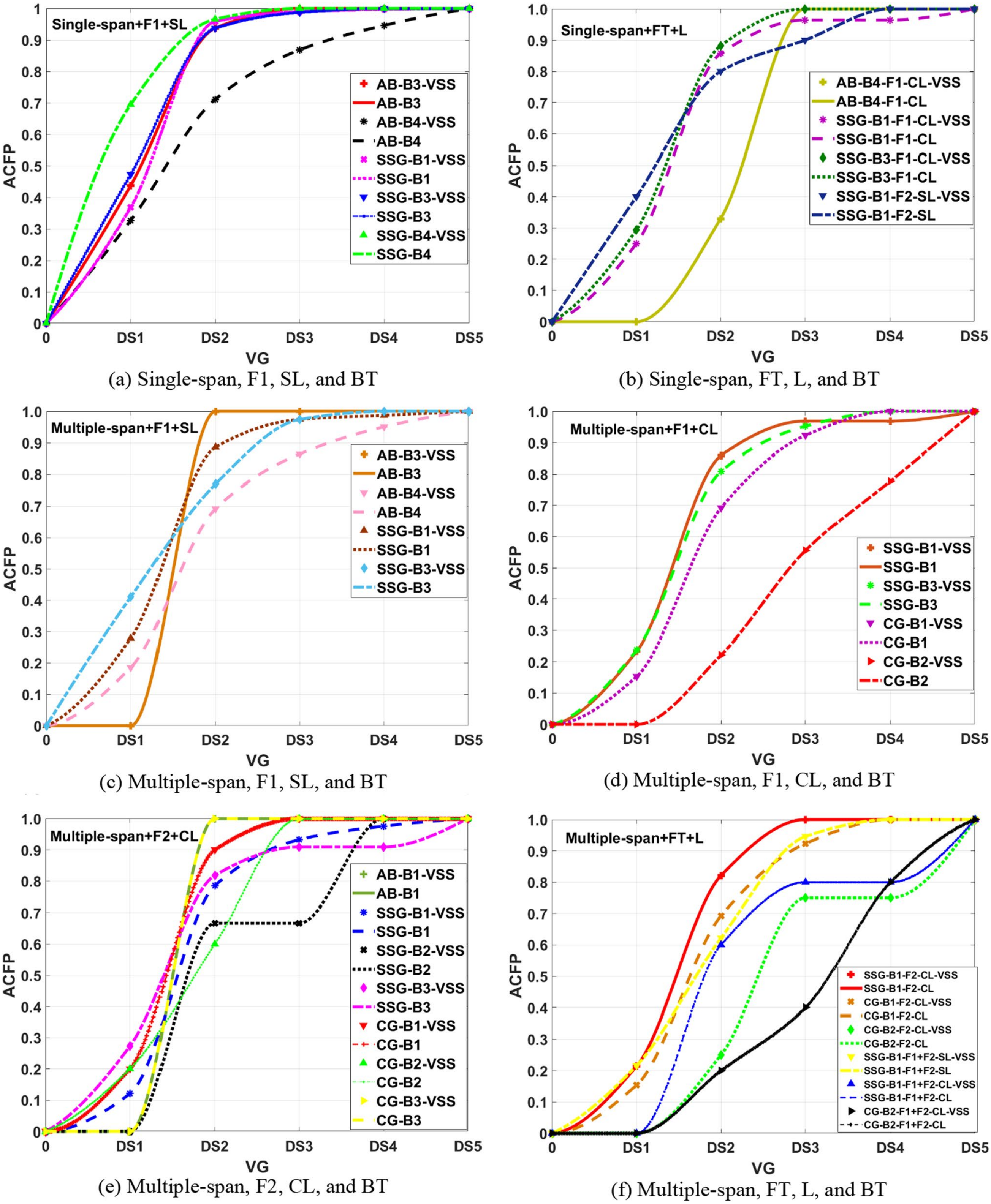

Fig. 16 Comparison of vulnerabilities of typical bridges based on coupled FT, L, S, and BT factors

vulnerability influencing factor, combined with nonlinear regression and the failure-exceedance probability model, the updated fragility regression model was established, and the vulnerabilities of typical bridges under the above single influencing factors were compared and analyzed. This led to the differences in vulnerability and seismic performance of various typical bridges under the influence of the above factors.

Combined with the actual seismic-damage observation, the vulnerabilities of SSG, CG, and AB under the influences of the coupled factors of (i) linear type and bridge length, (ii) pier type and foundation type, and (iii) foundation type, linear type, span, and bearing type were analyzed. Combined with the failure-exceedance probability model, the vulnerability point cloud, plane, surface, and curve model considering the above coupling factors was established, and a comparative analysis was performed. Finally, the vulnerability differences of typical structures based on the coupled influencing factors were developed, and suggestions were made to improve their seismic performance. Based on the analysis of the vulnerabilities of typical bridges under the influences of single and coupled factors, the vulnerability probability model of the whole Wenchuan earthquake region was established.

The conclusions can be used for the damage assessment and prediction of the empirical seismic damage of typical bridges and provide the necessary theoretical and practical reference for the revision of bridge seismic codes and seismic intensity scales. According to the actual seismic damage survey data, the bridge vulnerability is affected by the coupling of multiple factors in different intensity regions. Considering the macrointensity parameters to evaluate bridge vulnerability under the influence of various aspects will be the focus of this study. The research results obtained can provide a reasonable reference for reviewing typical intensity zoning and verifying regional macrointensity levels in bridge damage assessments.

Acknowledgements The basic data of this study were derived from the earthquake loss observation database of the China Earthquake Administration (CAE) and the Wenchuan earthquake loss observation team of the Institute of Engineering Mechanics of CAE. The research described in this study was financially supported by the Basic Scientific Research Business Expenses of Provincial Universities in Heilongjiang Province (Special Plan of Heilongjiang University (2022-1056)) and a project funded by Heilongjiang Postdoctoral Science Foundation (LBH-Z22294), China.

Data availability Some or all data, models, or codes that support the findings of this study are available from the corresponding author upon reasonable request.

Declarations

Conflict of interest The authors declare that they have no conflicts of interest.

Ethical approval It is stated that the study was performed based on ethical standards.

References

1. Booker NK, Clegg RE, Knights P, Gates JD. The need for an internationally recognised standard for engineering failure analysis. Eng Fail Anal. 2020;110:104357. https://doi.org/10.1016/j.engfailanal.2019.104357.
2. Shekhar S, Ghosh J. A metamodeling based seismic life-cycle cost assessment framework for highway bridge structures. Reliability Eng Syst Saf. 2020;195:106724. https://doi.org/10.1016/j.ress.2019.106724.
3. Ramadan OMO, Mehanny SSF, Kotb AAM. Assessment of seismic vulnerability of continuous bridges considering soil-structure interaction and wave passage effects. Eng Struct. 2020;206:110161. https://doi.org/10.1016/j.engstruct.2019.110161.
4. Li SS, Wei B, Tan H, Li CB, Zhao XM. Equivalence of friction and viscous damping in a spring-friction system with concave friction distribution. J Test Eval. 2021;49(1):372–95. https://doi.org/10.1520/JTE20190885.
5. Perdomo C, Monteiro R, Sucuoğlu H. Development of fragility curves for single-column RC Italian bridges using nonlinear static analysis. J Earthquake Eng. 2020;26(5):2328–52. https://doi.org/10.1080/13632469.2020.1760153.
6. Cademartori M, Sullivan TJ, Osmani S. Displacement-based assessment of typical Italian RC bridges. Bull Earthq Eng. 2020;18(9):4299–329. https://doi.org/10.1007/s10518-020-00861-9.
7. Padgett JE, DesRoches R. Methodology for the development of analytical fragility curves for retrofitted bridges. Earthquake Eng Struct Dyn. 2008;37:1157–74. https://doi.org/10.1002/eqe.801.
8. Li SQ, Liu HB. Vulnerability prediction model of typical structures considering empirical seismic damage observation data. Bull Earthq Eng. 2022;20:5161–203. https://doi.org/10.1007/s10518-022-01395-y.
9. Soleimani F. Propagation and quantification of uncertainty in the vulnerability estimation of tall concrete bridges. Eng Struct. 2020;202:109812. https://doi.org/10.1016/j.engstruct.2019.109812.
10. Bhuiyan MAR, Alam MS. Seismic vulnerability assessment of a multi-span continuous highway bridge fitted with shape memory alloy bars and laminated rubber bearings. Earthq Spectra. 2012;28(4):1379–404. https://doi.org/10.1193/1.4000089.
11. Kappos AJ, Manolis GD, Moschonas IF. Seismic assessment and design of R/C bridges with irregular congiguration, including SSI effects. Eng Struct. 2002;24(10):1337–48. https://doi.org/10.1016/S0141-0296(02)00068-8.
12. Agalianos A, Sieber M, Anastasopoulos I. Cost-effective analysis technique for the design of bridges against strike-slip faulting. Earthquake Eng Struct Dyn. 2020;49(11):1137–57. https://doi.org/10.1002/eqe.3282.
13. Tong T, Lei H, Yuan S, Liu Z. Experimental investigation and seismic vulnerability assessment of low flexural strength rectangular bridge piers retrofitted with ultrahigh-performance

concrete jackets. Eng Struct. 2020;206:110132. https://doi.org/10.1016/j.engstruct.2019.110132.
14. Attary N, Symans M, Nagarajaiah S, Reinhorn AM, Constantinou MC, Sarlis AA, Pasala DTR, Taylor DP. Experimental shake table testing of an adaptive passive negative stiffness device within a highway bridge model. Earthq Spectra. 2015;31(4):2163–94. https://doi.org/10.1193/101913EQS273M.
15. Li SQ, Liu HB. Comparison of vulnerabilities in typical bridges using macroseismic intensity scales. Case Stud Constr Mater. 2022;16:e01094. https://doi.org/10.1016/j.cscm.2022.e01094.
16. Lew SW, Wotherspoon L, Hogan L, Ai-Ani M, Chigullapally P, Sadashiva V. Assessment of the historic seismic performance of the New Zealand highway bridge stock. Struct Infrastruct Eng. 2020;17(5):689–701. https://doi.org/10.1080/15732479.2020.1762675.
17. Li SQ, Chen YS, Liu HB, Du K. Empirical seismic fragility rapid prediction probability model of regional group reinforced concrete girder bridges. Earthquakes Struct. 2022;22(6):609–23. https://doi.org/10.12989/eas.2022.22.6.609.
18. Padgett JE, DesRoches R, Nilsson E. Regional seismic risk assessment of bridge network in Charleston, South Carolina. J Earthquake Eng. 2010;14:918–33. https://doi.org/10.1080/13632460903447766.
19. Li SQ, Liu HB, Farsangi EN, Du K. Seismic fragility estimation considering field inspection of reinforced concrete girder bridges. Struct Infrastruct Eng. 2023. https://doi.org/10.1080/15732479.2023.2208565.
20. Li SQ. Empirical resilience and vulnerability model of regional group structure considering optimized macroseismic intensity measure. Soil Dyn Earthquake Eng. 2023;164:107630. https://doi.org/10.1016/j.soildyn.2022.107630.
21. Li SQ, Chen YS, Yu TL. Comparison of macroseismic intensity scales by considering empirical observations of structural seismic damage. Earthq Spectra. 2021;37(1):449–85. https://doi.org/10.1177/8755293020944174.
22. Li SQ, Liu HB. Analysis of probability matrix model for seismic damage vulnerability of highway bridges. Geomat Nat Haz Risk. 2022;13(1):1395–421. https://doi.org/10.1080/19475705.2022.2077146.
23. Li SQ, Chen YS. Vulnerability and economic loss evaluation model of a typical group structure considering empirical field inspection data. Int J Disaster Risk Reduct. 2023;88:103617. https://doi.org/10.1016/j.ijdrr.2023.103617.
24. GB/T 17742. (2020) The Chinese seismic intensity scale. (In Chinese)
25. Li SQ, Chen YS, Liu HB, Del Gaudio C. Empirical seismic vulnerability assessment model of typical urban buildings. Bull Earthq Eng. 2023. https://doi.org/10.1007/s10518-022-01585-8.
26. GB/T 24336 (2009) Classification of earthquake damage to lifeline engineering. (In Chinese)
27. Li SQ, Chen YS. Analysis of the probability matrix model for the seismic damage vulnerability of empirical structures. Nat Hazards. 2020;104(1):705–30. https://doi.org/10.1007/s11069-020-04187-2.
28. JTG/TB02-01 (2008) Guidelines for seismic design of highway bridges. (In Chinese)
29. JTG/T 2231-01. (2020) Specifications for seismic design of highway bridges. (In Chinese)
30. GB/T 17742 (2008) The Chinese seismic intensity scale. (In Chinese)
31. Li SQ. Comparison of RC girder bridge and building vulnerability considering empirical seismic damage. Ain Shams Eng J. 2023. https://doi.org/10.1016/j.asej.2023.102287.
32. Li SQ. Empirical vulnerability estimation models considering updating the structural earthquake damage database. Soil Dyn Earthquake Eng. 2023. https://doi.org/10.1016/j.soildyn.2023.107864.
33. Formisano A, Chieffo N. Seismic damage scenarios induced by site effects on masonry clustered buildings: a case study in south Italy. Int J Architect Herit. 2022. https://doi.org/10.1080/15583058.2022.2104143.
34. Chieffo N, Clementi F, Formisano A, Lenci S. Comparative fragility methods for seismic assessment of masonry buildings located in Muccia (Italy). J Build Eng. 2019;25:100813. https://doi.org/10.1016/j.jobe.2019.100813.
35. Li SQ, Gardoni P. Empirical seismic vulnerability models for building clusters considering hybrid intensity measures. J Build Eng. 2023;68:106130. https://doi.org/10.1016/j.jobe.2023.106130.
36. Chen LS, Zhuang WL, Zhao QH. Report on highways damage in the Wenchuan earthquake. Beijing: China Communications Press; 2012.
37. Li SQ, Chen YS, Liu HB, Du K, Chi B. Assessment of seismic damage inspection and empirical vulnerability probability matrices for masonry structure. Earthquakes Struct. 2022;22(4):387–99. https://doi.org/10.12989/eas.2022.22.4.387.
38. Li SQ, Liu HB, Du K, Han JC, Li YR, Yin LH. Empirical seismic vulnerability probability prediction model of RC structures considering historical field observation. Struct Eng Mech. 2023;86(4):547–71. https://doi.org/10.12989/sem.2023.86.4.547.
39. Del Gaudio C, Martino GD, Ludovico MD, Manfredi G, Prota A, Ricci P, Verderame GM. Empirical fragility curves from damage data on RC buildings after the 2009 L'Aquila earthquake. Bull Earthq Eng. 2017;15:1425–50. https://doi.org/10.1007/s10518-016-0026-1.
40. Li SQ. Comparison of empirical structural vulnerability rapid prediction models considering typical earthquakes. Structures. 2023;49:377–401. https://doi.org/10.1016/j.istruc.2023.01.130.